Tectonic Setting and Provenance of the Neoproterozoic Uinta Mountain and Big Cottonwood Groups, Northern Utah: Constraints from Geochemistry, and Detrital Modes

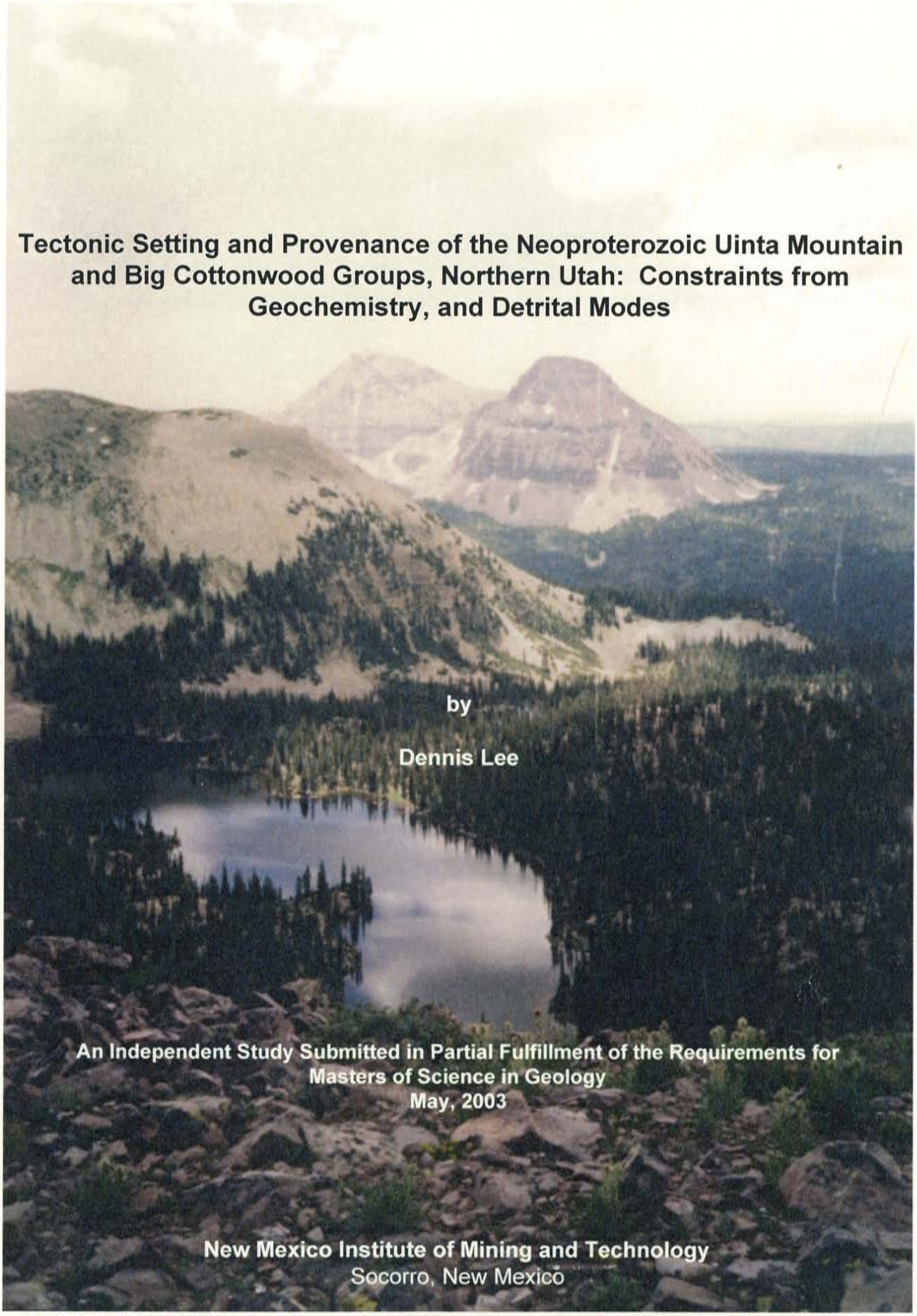

by

Dennis Lee

An Independent Study Submitted in Partial Fulfillment of the Requirements for
Masters of Science in Geology
May, 2003

New Mexico Institute of Mining and Technology
Socorro, New Mexico

Tectonic Setting and Provenance of the Neoproterozoic Uinta Mountain and Big Cottonwood Groups, Northern Utah: Constraints from Geochemistry, and Detrital Modes

by

Dennis Lee

An Independent Study Submitted in Partial Fulfillment of the Requirements for
Masters of Science in Geology
May, 2003

New Mexico Institute of Mining and Technology
Socorro, New Mexico

Abstract

The Neoproterozoic Uinta Mountain Group was deposited in an east-trending intracratonic rift bounded on the north by an active fault system and opening into a shallow sea on the west where the Big Cottonwood Group was deposited in an estuary. Although this rift may have been associated with the early stages in the breakup of Rodinia, it was not an aulacogen. Geochemical and detrital mode studies indicate that Uinta Mountain Group sediments were derived from mixed Archean and Paleoproterozoic sources with the former dominating. Big Cottonwood Group sediments appear to have been derived predominantly from Paleoproterozoic sources. The Archean sediment source is the Wyoming craton, and source rocks comprised dominantly granites enriched in Th, U, Y, Zr, Hf, and REE. The relative abundance of enriched granite implied by sedimentary rocks of the Uinta Mountain Group indicates that the Wyoming craton is anomalous compared to other Archean cratons.

CIA values and A-CN-K relationships in shales of the Uinta Mountain and Big Cottonwood groups indicate high degrees of weathering of sources, probably in subtropical to tropical climates supporting a near-equatorial location for southwestern Laurentia at about 800 Ma. Differences in the Nd isotopic composition between the Big Cottonwood Group and Neoproterozoic sedimentary rocks in western Utah and northeast Nevada suggest a northwestern striking uplift in northwest Utah, possibly ancestral to the Paleozoic Toole-Uinta arch.

Table of Contents

List of Figures

List of Tables

Introduction

Detrital sediments are a primary source of information about continents. The tectonic, climatic, and magmatic history of the past must be, in some cases, determined entirely through their sedimentary remains. Extracting this information may involve several approaches, such as establishing lithologic association (petrotectonic assemblage), determining chemical and isotopic composition, and identifying and describing detrital mineralogy (Dickinson et al., 1983; Taylor and McLennan, 1985; Roser and Korsch, 1988 McLennan et al., 1993). Crust that is not accessible because of erosion, or burial by ice or younger deposits can only be investigated indirectly through detrital sediments. Detrital modes, trace elements, Nd and Pb isotopes, and U/Pb detrital zircon ages can be used to examine sediment provenance (Taylor and McLennan, 1985; Sawyer, 1986; Condie and Wronkiewicz, 1990; Crichton and Condie, 1993; Condie, 1993; McDaniel et al., 1994; Farmer and Ball, 1997). Paleoclimatic characterization of source regions can be deduced by assessing the amount of chemical weathering, using elements such as Na, Ca, and Sr that are rapidly removed during chemical weathering (Nesbitt and Young, 1996; Nesbitt et al., 1997).

The early breakup history of the Mesoproterozoic supercontinent Rodinia has gained much interest among researchers recently, and the primary source of information about this event is recorded in sediments deposited in basins formed during the early stages of breakup about 800 Ma (Farmer and Ball, 1997). This study used combined field, detrital mode, and geochemical analyses of Neoproterozoic

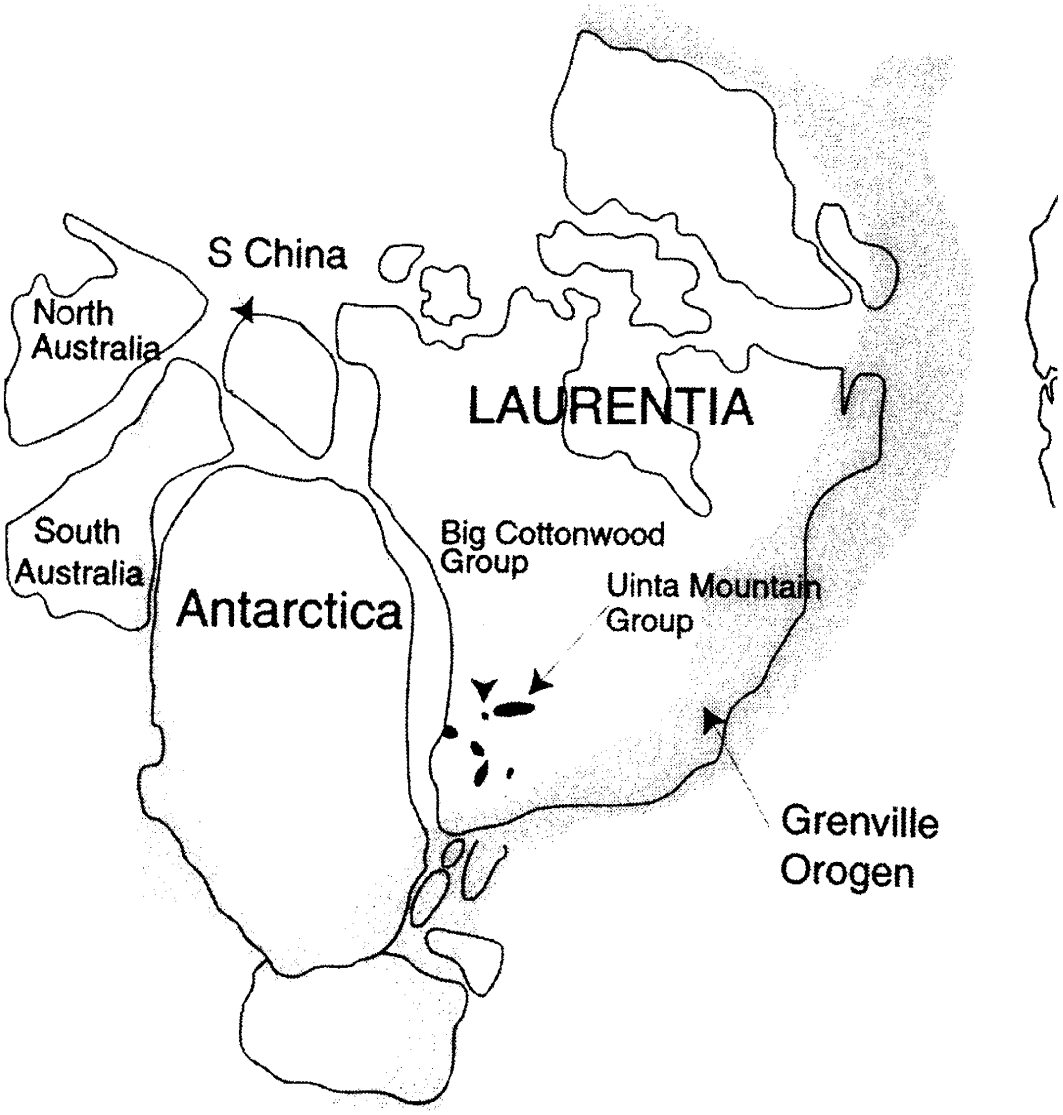

Fig 1: Index map showing the locations of the Uinta Mountain and Big Cottonwood Groups and other Neo-Mesoproterozoic basins in Southwestern Laurentia, as part of the Neoproterozoic supercontinent Rodinia about 800 Ma (after Powell et al., 1994; Dalziel, 1997).

sedimentary rocks from the Uinta Mountain and Big Cottonwood groups in northern Utah (Fig. 1). Information about the origin and provenance of these deposits will lead to a more complete understanding of the history of southwestern Laurentia and the breakup of Rodinia.

Geologic Overview

The Uinta Mountain Group is a thick succession of marine, silicilastic, mostly fluvial sediments exposed in an east-trending basin in northeastern Utah and northwestern Colorado (Figs. 1, 2). Micropaleontologic and paleomagnetic results from the Uinta Mountain Group suggest that it was deposited in the Neoproterozoic (1000-700 Ma) and that it is broadly correlative with the Pahrump Group in the Death Valley area of California and Chuar Group in the Grand Canyon of Arizona (Vidal, 1985; Link et al., 1993). The Uinta Mountain Group basin approximately follows the suture zone between the Archean Wyoming craton on the north and accreted Paleoproterozoic arc terranes on the south (Condie, 1992; Ball and Farmer, 1998). In the western Uinta Mountains where this investigation is focused, the succession of rocks in the Uinta Mountain Group includes quartz arenite, siltite, arkose, shale, and minor conglomerate (Wallace and Crittenden, 1969; Sanderson, 1984; Link et al., 1993). Although the succession ranges to more than 7 km thick, it averages about 4 km. Lithologic proportions vary with sedimentary facies, but overall quartz arenite (including feldspathic quartz arenite and subarkose) dominates (65%), with subordinate shale/siltstone (20%) and arkose (15%). These sedimentary rock types occur throughout the stratigraphic section in the western Uinta Mountains, and only the Red Pine Shale is composed predominantly of siltite and shale. The Uinta Mountain Group is thickest along the northern margin of the basin; this asymmetry may be controlled by faulting along its northern boundary (Sanderson, 1984).

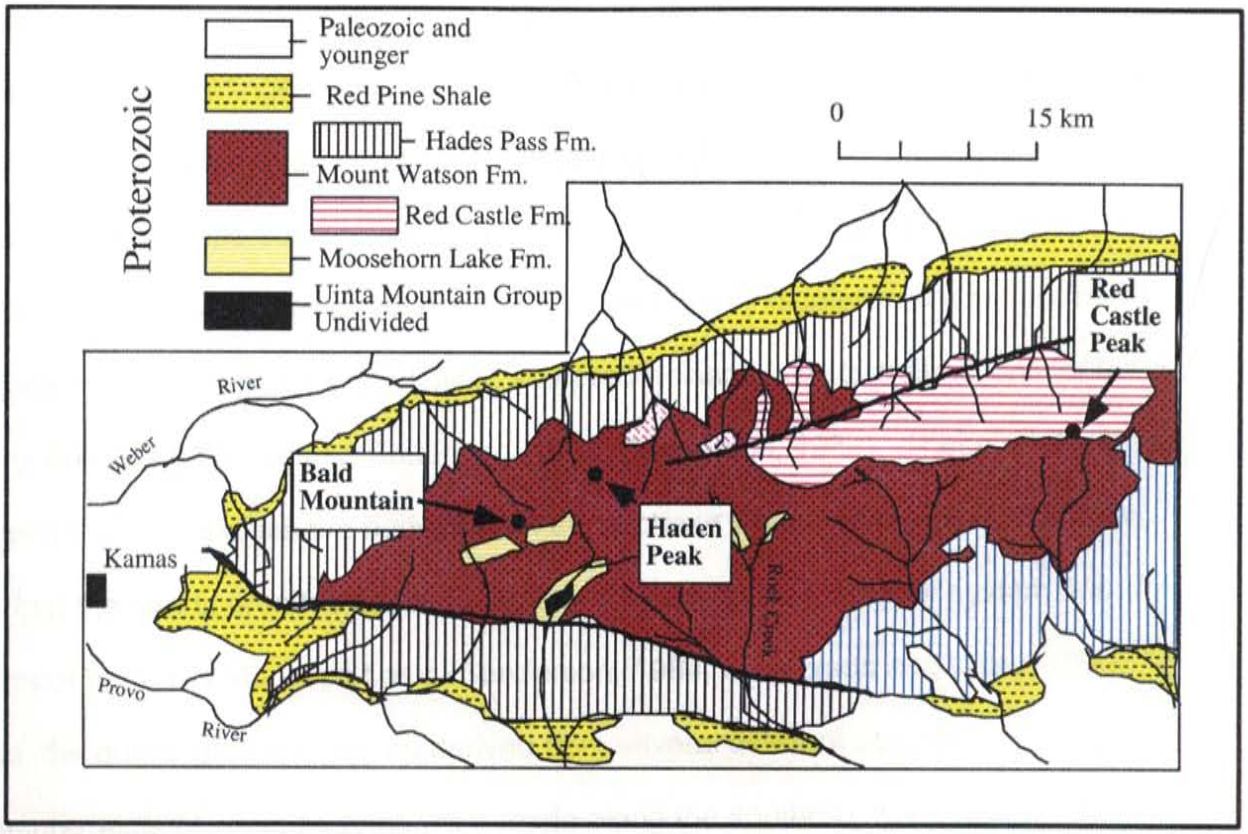

Fig. 2: Generalized geologic map and stratigraphic column of the units of the Uinta Mountain Group (Sanderson, I.D. 1979).

The oldest rocks in the Uinta Mountain Group, exposed in some of the deeper canyons in the western Uinta Mountains (undivided Uinta Mountain Group), are composed of very pure quartz arenite (Fig. 2). These rocks are overlain by several formations that interfinger with each other, the youngest of which is the Red Pine Shale. Relatively well-sorted quartz arenite is interbedded with arkose and minor shale in most formations, the proportions of various lithologies varying from location to location. Cross-bedding is well-preserved in the sandstones, and indicates south to southwest paleocurrent directions for the arkoses, and predominantly western directions for the quartz arenites (Wallace and Crittenden, 1969; Sanderson, 1984). These relationships suggest that the arkoses are derived from the Archean Wyoming craton on the north, and that the quartz arenites are deposited by a westward-flowing river system near the center of the Uinta Mountain basin (Sanderson, 1984; Sanderson and Wiley, 1986). Thus, the quartz arenites may be derived from several different sources. Measurements of cross-bedding were made along the southern side of the Uinta Mountains to test for southern sources (Fig. 3a, b, c). The measurements suggest paleocurrent directions in this region that range from west to south, and thus no evidence is found for southern sediment sources.

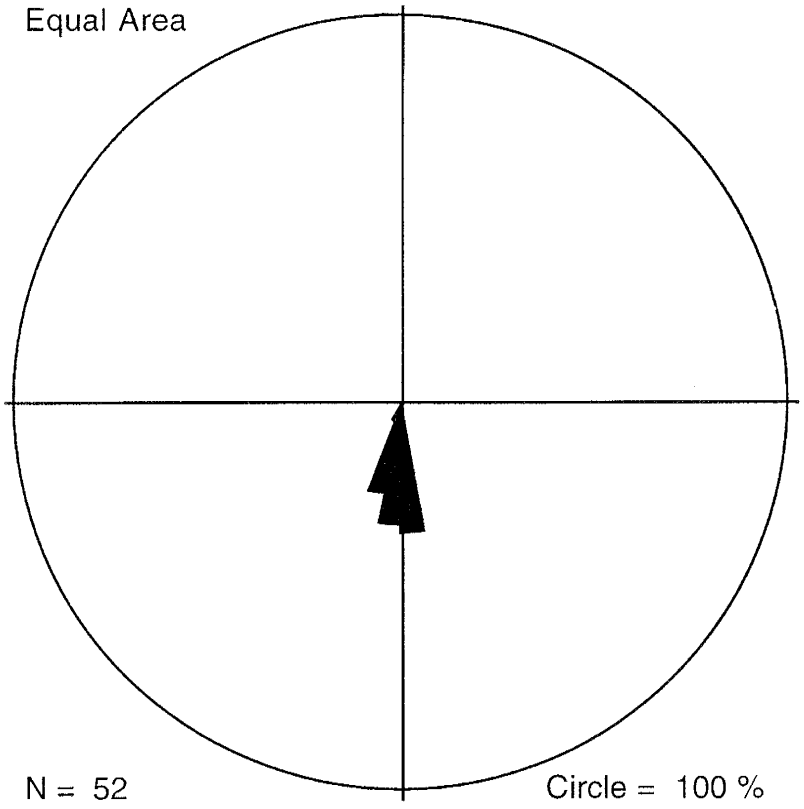

Fig. 3a: Rose diagram of strike and dips from cross bedding in the Hades Peak Formation at Iron Mine Creek, southern flank of the Uinta Mountains. Iron Mine Creek is the most westerly of the areas where cross-bedding was measured.

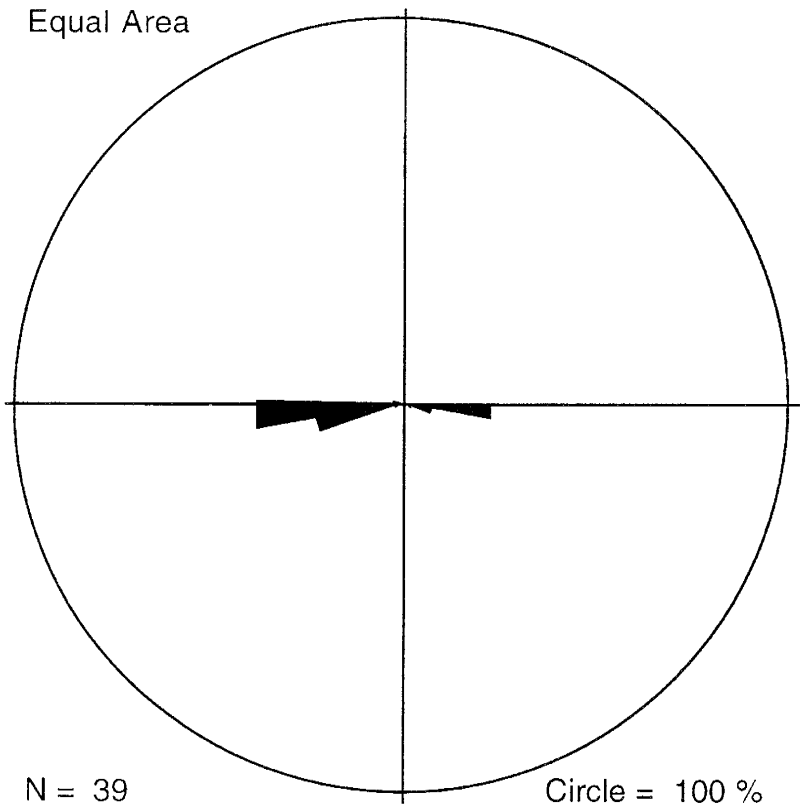

Fig. 3b: Rose diagram of strike and dips from cross bedding in the Hades Peak Formation at Stillwater Dam, southern flank of the Uinta Mountains.

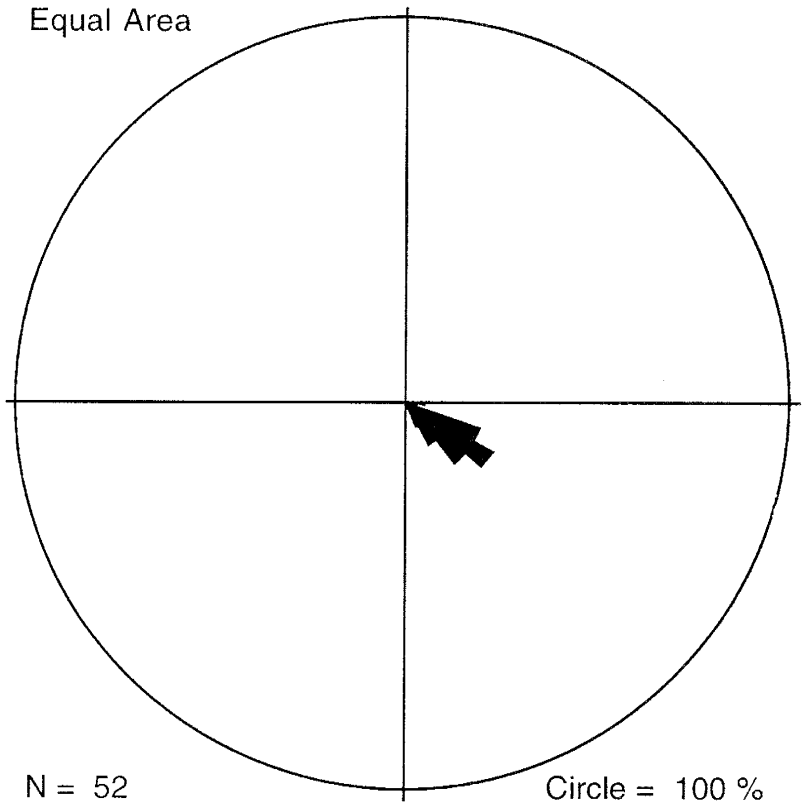

Fig. 3c: Rose diagram of strike and dips from cross bedding in the Hades Peak Formation at Moon Lake, southern flank of the Uinta Mountains. Moon Lake is the most easterly of the areas where cross-bedding was measured.

The Big Cottonwood Group east of Salt Lake City generally is correlated with the Chuar Group in the Grand Canyon and also with the Uinta Mountain Group to the east (James, 1979; Link et al., 1993). The Big Cottonwood Group is composed of up to 5 km of interbedded quartz arenite, siltite, and shale deposited in a shallow marine environment, in part an estuary, at the mouth of the basin in which the Uinta Mountain Group was deposited (Chan et al., 1994; Ehlers et al, 1997; Ehlers and Chan, 1999). Tidal rhythmites described in the Big Cottonwood Group suggest seasonal climatic changes based on the identification of both daily and monthly events. Five distinct lithofacies have been identified in the Big Cottonwood Group and cross-bedding indicates westward paleotransport. These sediments were probably carried by rivers from the east that deposited the Uinta Mountain Group (Ehlers et al., 1997).

Sampling and Analytical Methods

Over 100 samples of sedimentary rocks were collected from the Uinta Mountain Group in the western Uinta Mountains and from the Big Cottonwood Group in Big Cottonwood Canyon (Fig. 1, 2). Of these, 52 were selected for chemical analysis by X-ray fluorescence (XRF) and instrumental neutron activation (INAA). Samples were coarsely crushed with a steel jaw crusher and then pulverized to coarse sand with a Bico pulverizer, using porcelain plates. An aliquot of the coarse sand to be used for INAA was hand ground with a ceramic mortar and pestle, and another aliquot for XRF was ground to a fine powder in a steel swing mill.

Major and trace elements including Ba, Nb, Ni, Pb, Rb, Sr, V, Y, and Zr were analyzed by XRF at New Mexico Tech. Fused disks were prepared using the methods described by Hallett and Kyle (1993). Pressed powder pellets were prepared using 7 grams of sample, mixed with a polyvinyl alcohol solution, and pressed to 10 tons with boric acid backing. Analyses were made with an automated Philips PW2400 XRF spectrometer and Philips PC software following the procedures described in Hallett and Kyle (1993). Precision and detection limits for both XRF and INAA are also discussed in this reference.

Trace elements including Sc, Cr, Co, La, Ce, Nd, Sm, Eu, Tb, Yb, Lu, Hf, Ta, Th and U were analyzed by INAA at New Mexico Tech following the methods of Hallett and Kyle (1993). Approximately 80 mg of each sample powder was sealed in ultrapure suprasil glass vials and irradiated at the Research Reactor Facility University of Missouri for 30 hours at a flux of 2.4×10^{13} n cm^{-2} sec^{-1}. Samples were analyzed with

two high-purity Ge detectors (resolution 1.85 keV @ 1332 keV, efficiency 25%) using a Nuclear Data 9900 system with a VAX station computer. Counts were made 6 to 12 days after irradiation and again at 35-45 days after irradiation. A NIST standard fly ash (SRM1633a) was used for calibration.

Petrographic Features

Fine- to medium-grained quartz and feldspathic arenites comprise 60-70% of the Uinta Mountain Group, and consist mainly of moderately to well-sorted monocrystalline quartz. Detrital feldspars comprise up to about 10% of feldspathic quartz arenites. Minor heavy detrital phases include magnetite, apatite, and zircon. Quartzites are cemented with quartz, typically in optical continuity with adjacent grains, with hematite and clay cements of negligible importance. Medium and coarser sands are typically well-rounded and commonly possess silica overgrowths.

Most of the overgrowths, which comprise up to 45% of the quartz sand grains in the Mt. Watson Formation, were interpreted by Sanderson (1979; 1984) as inherited overgrowths from older, reworked sediments. This petrographic study, however, indicates that most or all of the quartz overgrowths in all formations in the western Uinta Mountain Group are primary quartz overgrowths formed during diagenesis (Fig 4). Cementation with interlocking quartz overgrowths, in optical continuity, is ubiquitous throughout the samples studied, supporting this interpretation. Authigenic overgrowths are usually interlocking, with long contacts, and occur on most of the grains in a slide, no matter the shape of the nucleus (Folk, 1974).

Arkose samples in this study show some difference in cementation and matrix than the predominant quartz cementation. Lithologies with predominantly polycrystalline metaquartz, and significant feldspar content show no quartz cementation, but contain clay matrices, possibly from altered feldspars.

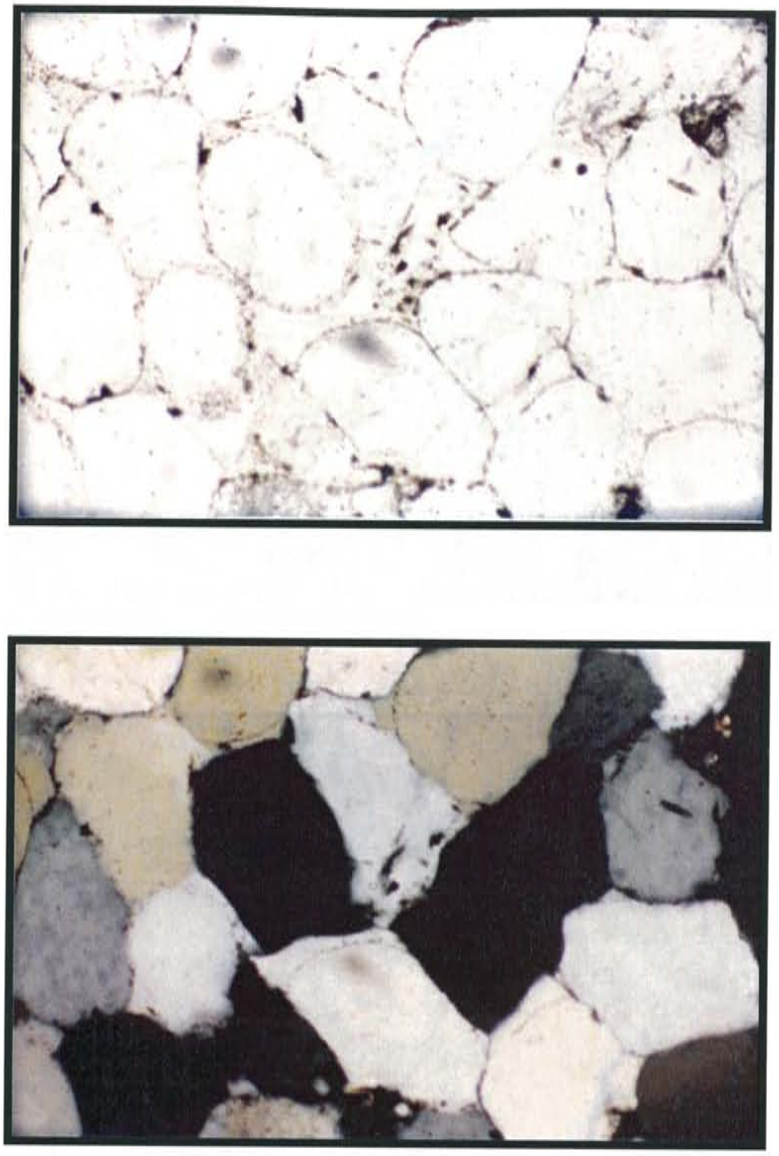

Fig 4. Quartz arenite from the Hades Peak formation of the Uinta Mountain Group (HP-4). Quartz grains are well rounded. Quartz overgrowths have interlocking boundaries, and are in optical continuity with grains. Quartz grains show signs of compression during burial diagenesis, such as elongated grain-to-grain contact, and distortion of rounded shape. This sample is representative of quartz arenites throughout the study area. Plain and polarized light; scale x50.

A)

B)

Fig 5. A) Quartz arenite shown in Fig. 1 (HP-4), displaying relatively large plagioclase grain in contrast with finer grained quartz. Polarized; scale x50. B) Quartz arenite (MW-41) with relatively larger K-feldspar, with the grain on the right displaying perthitic texture. Polarized; scale x50.

One sample, Hades Peak #2, has 10% calcite cement, secondary to quartz cement, and appears to have been void infilling rather than replacement of quartz cement. Sample #2 of the Mt. Watson formation has hematite cementation, unique among the samples of this study.

As stated above, quartz arenites contain up to 10% feldspars, with significant grain size differences between samples (Fig. 5), the feldspars being significantly larger than the quartz grains. Plagioclase and K-feldspars are found in quartz arenites, but both are consistently much larger than quartz grains found in the samples.

In general, arkose is coarser grained (typically medium to coarse sand) than associated quartz arenite. Some samples are very coarse and grade into pebble conglomerates in which chert, fine-grained quartz arenite, and granitoids dominate the clast assemblage (Fig 6). In contrast to quartz arenite, arkose is poorly sorted, contains angular to subangular typically polycrystalline quartz grains (Fig. 6), and is cemented with a combination of quartz, hematite, and clays. Although in most units K-feldspar is dominant, in some units well-twinned plagioclase dominates (Table 1).

The preservation of plagioclase in some of the arkoses indicates weathering, transportation, and burial of these sediments occurred quite rapidly (Fig. 7). Detrital muscovite and biotite are common in some arkoses, and minor phases include magnetite, apatite, and zircon. Although some detrital feldspars are partially replaced with secondary clays, carbonate, and iron oxides, generally feldspars are well-preserved, and thus the rocks should give accurate detrital modes.

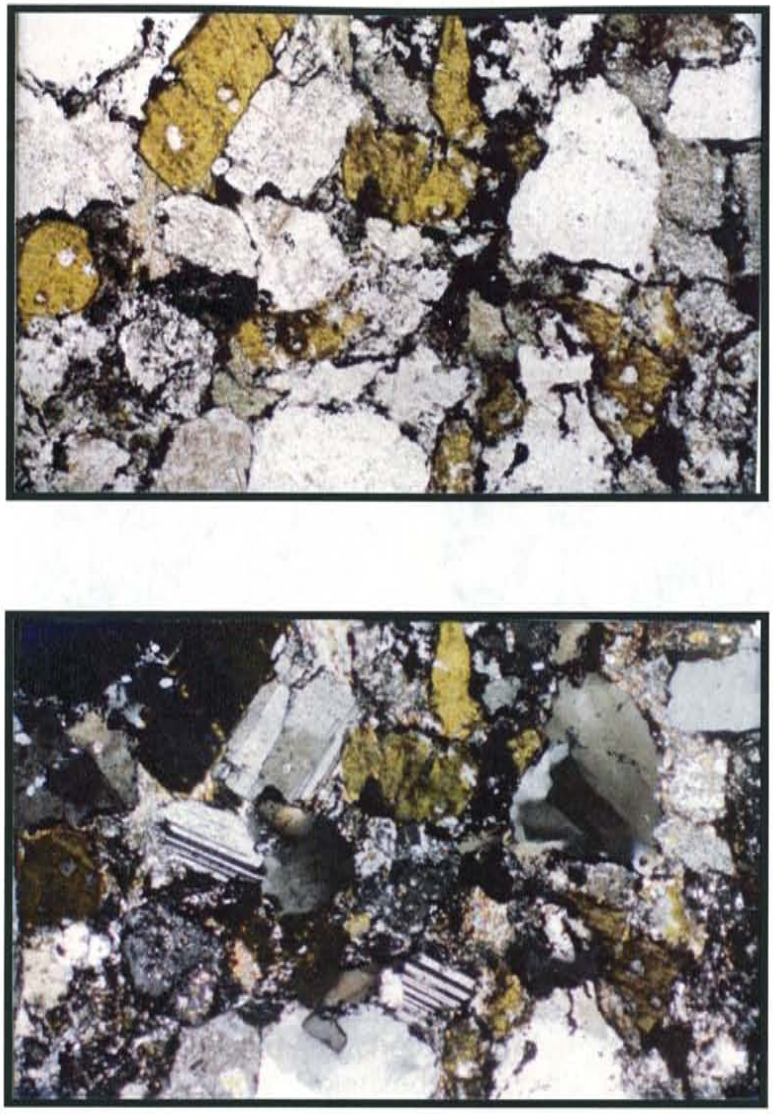

Fig 6. Arkose from the Red Castle formation of the Uinta Mountain Group (RC-7). Well-preserved plagioclase displays twinning in some grains, and minor clay alteration in others. Thin sections were stained for K-feldspar, and these grains stand out because they are relatively large, angular, and yellow-brown. Quartz grains have undulate extinction. Plain and polarized light; scale x50.

Fig. 7. (MW-48) Polycrystalline quartz grains and plagioclase altered to sericite, with clays and stretched and deformed micas comprising the matrix. Polarized; scale x50.

No evidence was found for large amounts of feldspar or rock fragment replacement, which can destroy original modes (Helmold, 1985; Milliken, 1988). The incidence of polycrystalline quartz in rocks classified as quartz arenite is rare. In fact, monocrystalline quartz predominates in almost all samples described in this study.

Siltstone and shale in the Uinta Mountain and Big Cottonwood groups vary from thin bedded to fissile, and range from maroon to gray, green, or black in color. X-ray diffraction studies of powdered whole-rock shale samples from the Red Pine Shale indicate that quartz, illite (including sericite), and chlorite dominate, with variable but smaller amounts of iron oxides (limonite, hematite) quartz, and K-feldspar (Table 2). Kaolinite has also been reported from some shales in the Mt. Watson Formation (Sanderson, 1979).

Table 1. Modal Analysis of thin section derived from point counts consisting of 500 points per thin section.

	Qm	Qp	K	P	L	Qm/F	K/P
MW-24	25	26	19	30	1	1	1
MW-10	83	1	12	4	0	5	3
MW-12	97	0	2	1	0	30	2
MW-48	16	40	1	41	3	0	0
MW-2	34	9	13	43	2	1	0
MW-49	100	0	0	0	0		
MW-21	90	0	4	2	3	14	2
MW-11	53	12	22	10	3	2	2
MW-41	81	8	8	3	0	7	3
MW-27	97	1	0	2	0	55	
MW-37	91	2	4	3	0	14	1
HP-5	96	2	1	0	1	77	4
HP-21	91	2	3	1	4	22	2
HP-31	49	14	5	30	3	1	0
HP-25	78	3	1	7	11	9	0
HP-24	60	13	18	9	0	2	2
HP-14	98	2	0	0	0		
HP-22	95	1	0	0	4	395	
HP-13	40	15	26	18	0	1	1
HP-4	96	0	4	0	0	26	14
HP-18	92	1	6	2	0	12	4
HP-2	94	2	0	4	0	24	0
RC-7	27	14	26	33	1	0	1
RC-2	26	28	20	26	0	1	1
RC-9	96	1	1	3	0	26	0
RC-10	91	1	5	3	0	11	2
UMG-2	98	1	0	1	0	98	
UMG-1	100	0	0	0	0		
UMG-3	99	0	0	1	0	79	

Qm- Quartz monocrystalline
Qp – Quartz polycrystalline
K – Potassium Feldspar
P – Plagioclase
L – Lithic fragments
Qm/F – Ratio of quartz monocrystalline to total feldspar
K/P – Ratio of plagioclase to lithic fragments

Table 2. XRD Analysis of shale samples from the Red Pine and Moosehorn Lake Shales.

NMBMMR X-RAY FACILITY
QUALITATIVE MINERALOGICAL REPORT FOR KENT CONDIE
APRIL 12, 1999

x = major phase. Relative intensity of most intense peak >30.
m = minor phase. Relative intensity of most intense peak > 7 and < 30
tr = trace phase. Relative intensity of most intense peak <7
? = possible phase but not confirmed by at least three peaks

- = not detected

Lab #	Sample #	Quartz	Mica	Chlorite	Alkali Feldspar	Plagioclase
99D09A	RP-1	x	m	m		x
99D09B	MHL-12	x	m	m		
99D10A	MHL 4	x	m	m		
99D12A	RP 19	x	tr	tr	tr	x

Detrital Modes

Detrital modes of sandstones have been useful in constraining tectonic setting using the approach of Dickinson et al. (1983). Detrital modes of a representative group of quartz arenite and arkose from the Uinta Mountain Group are given in Table 1. At least 500 points were counted on each thin section (stained for K-feldspar) using the Dickinson-Gazzi method, where variations in grain size are minimized by counting fine-grained lithic fragments only if they are larger than the matrix limit (0.0625 mm). Single crystals larger than this size are counted as mineral grains, whether they occur as separate clastic components or as part of polycrystalline grains. Lithic fragments are uncommon in most of the sandstones, and generally absent in quartz arenite (Table 1). However, some arkoses in the Hades Peak and Red Castle Formations contain up to 10% of fine-grained sedimentary rock fragments. These fragments are chiefly chert, with small amounts of shale and fine-grained quartz arenite. No volcanic fragments were found in any of the Uinta Mountain Group sandstones. Some of the pebble conglomerates, however, contain granitoid fragments.

After recalculating the quartz-feldspar-lithic fragment proportions to 100%, the QFL values are plotted on the Dickinson tectonic setting graph (Fig. 8). All of the quartz arenites fall in the craton interior or upper part of the transitional field, regardless of the formation they come from. As pointed out by Dickinson et al. (1983), sandstones plotting in these fields are mature sandstones derived from relatively low-lying granitoid sources, supplemented by recycled sands from associated platform or passive margin basins. However, the CIA results discussed later suggest intense paleoweathering of

the sources, an effect which can skew the sandstone modes toward the craton interior field. Hence, some of the sandstones may have had provenance in the recycled orogen field. The abundance of extremely well-rounded quartz grains, especially in the Mt. Watson Formation, is suggestive of eolian reworking prior to final deposition in the fluvial system. Arkoses typically plot in the transition or basement uplift fields, in agreement with the results of Schwab (1998). Only one sample from the Red Castle Formation falls in the recycled orogen field. The Qm/F ratio of the arkoses is < 5 and often < 1, which is similar to this ratio in granites, attesting to the immaturity of these sediments (Table 1). K/P ratios are typically < 1, but range up to 5 in some samples, reaching 14 in one sample (HP-4). Sediments falling in the basement uplift field generally reflect continental rift settings in which the source detritus is rapidly transported and buried, so as to preserve feldspars, especially plagioclase. Sediments with these characteristics can also be deposited in foreland basins and deeply dissected arcs, neither of which, however, are consistent with the probable geologic setting of the Uinta Mountain Group.

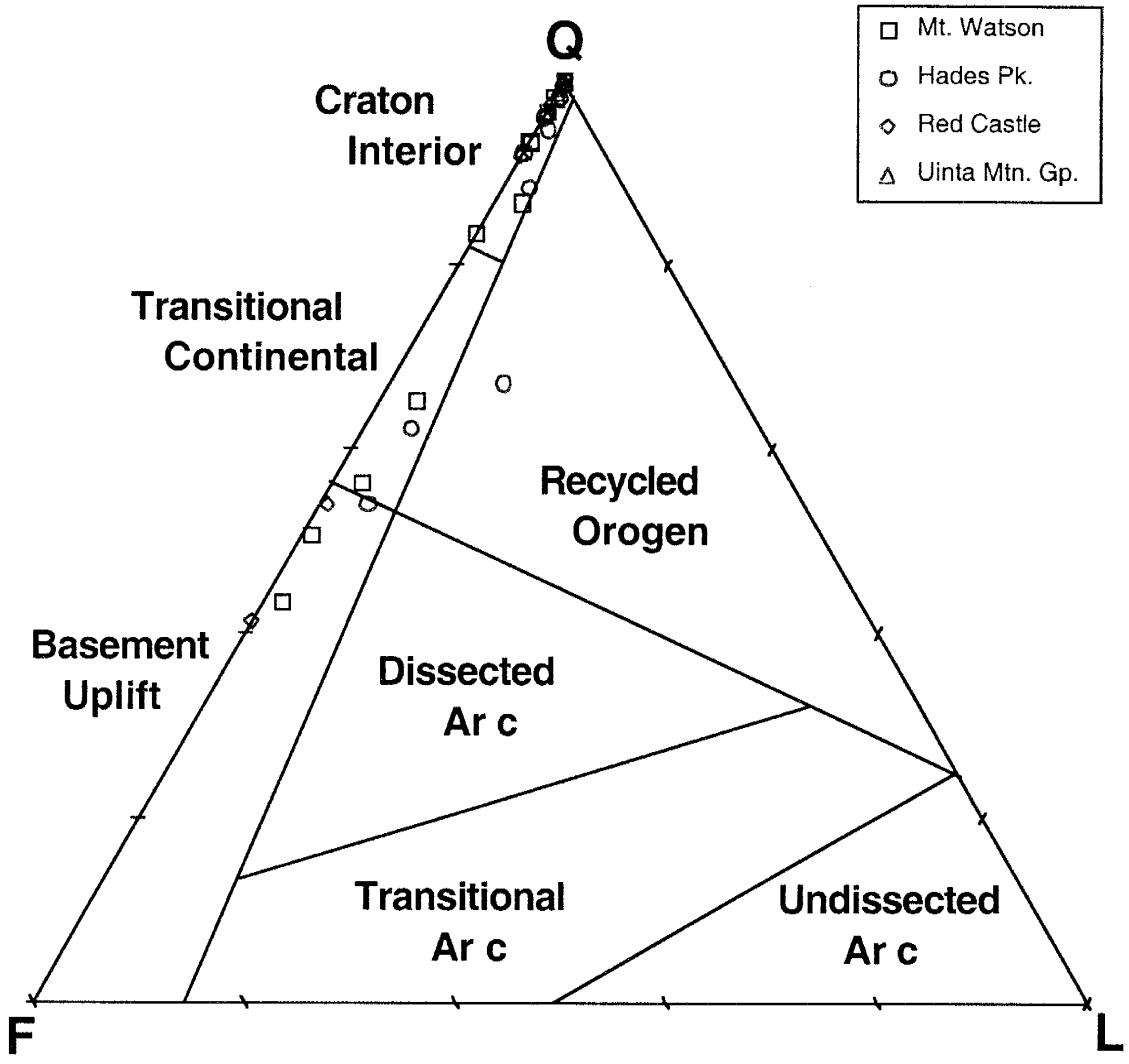

Fig. 8: QFL graph showing the distribution of quartz arenite and arkose from the Unita Mountain Group. Tectonic setting fields after Dickinson et al. (1983). Q = Qm + Qp; F = K + P; L = Ls. Data and definitions given in Table 1.

Geochemical Results

Major Elements

Detrital sediments from the Uinta Mountain Group define a linear trend on a SiO_2-Al_2O_3 graph, with shales containing less than about 70% SiO_2 and more than 10% Al_2O_3 (Fig. 9). Arkoses plot at an intermediate position and quartz arenites have > 90% SiO_2. Quartz arenites show two major populations: a large group with > 96% SiO_2 and sericite quartz arenites with 92-96 % SiO_2. One sample contains a large amount of iron oxide cement (HP-2). In general, the detrital sediments of the Uinta Mountain Group can be considered as mixtures of three components. The shales and quartz arenites are chiefly mixtures of illite (now mostly sericite) and quartz as also reflected by the modal minerals (Table 1). Arkose, on the other hand, can be considered as mixtures of quartz, illite, and K-feldspar, the latter of which also falls on the illite-quartz mixing line on the SiO_2-Al_2O_3 graph (Fig. 9).

Although data are somewhat scattered, there is a suggestion of a linear relation between MgO and Fe_2O_3T in the Uinta Mountain Group sediments (Fig. 10). Quartz and feldspar plot at the origin on this graph and biotite/chlorite fall at the other end of the array of points. In detail, shales seem to fall on a mixing line enriched in MgO relative to sandstones, which is consistent with their modal mineralogy (rich in clays and micas). Two of the BC samples (BC-2, 3) have unusually high Fe contents, falling off the Fe-Mg array, reflecting an abundance of iron oxide cement in these rocks (Fig. 10).

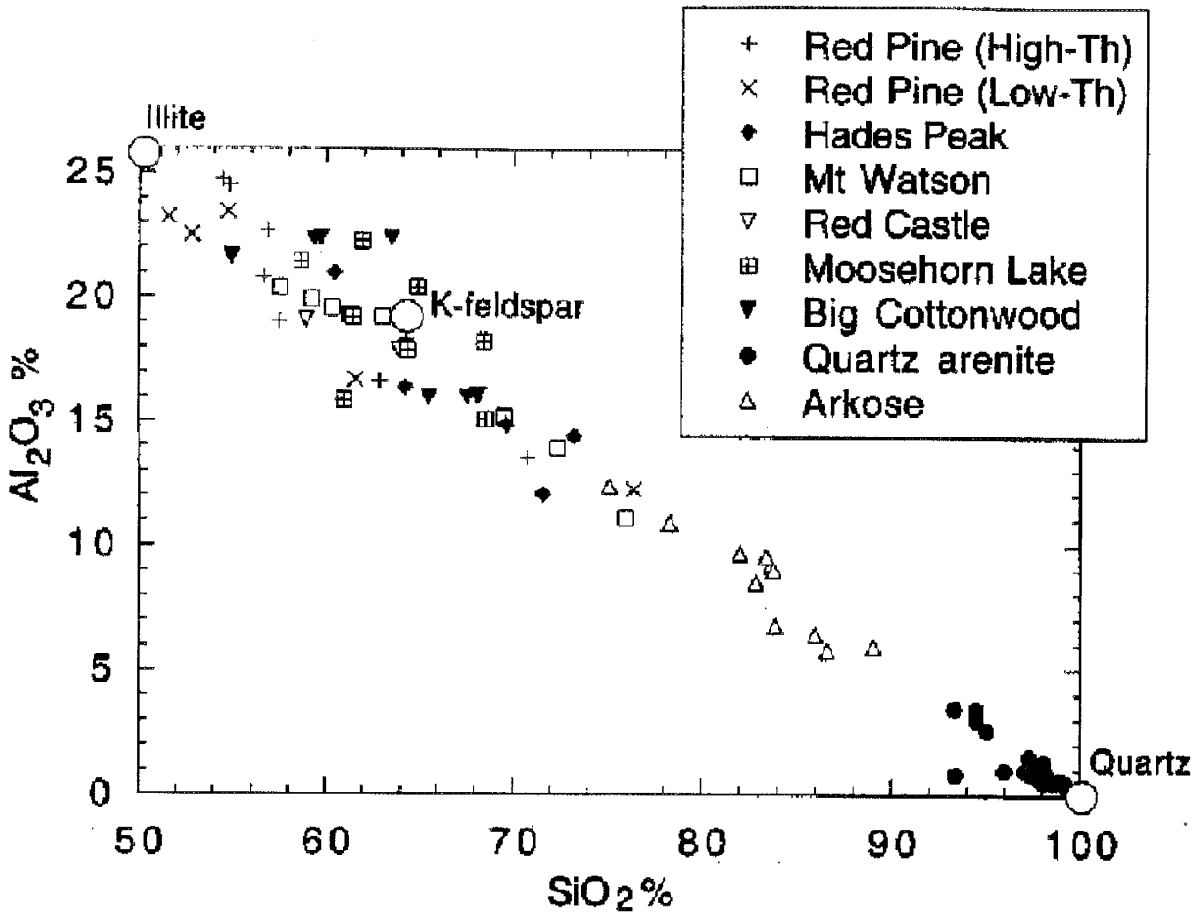

Fig. 9: Al_2O_3-SiO_2 graph showing the distribution of sediments from the Uinta Mountain and Big Cottonwood groups. All samples with formation names are shales and siltstones.

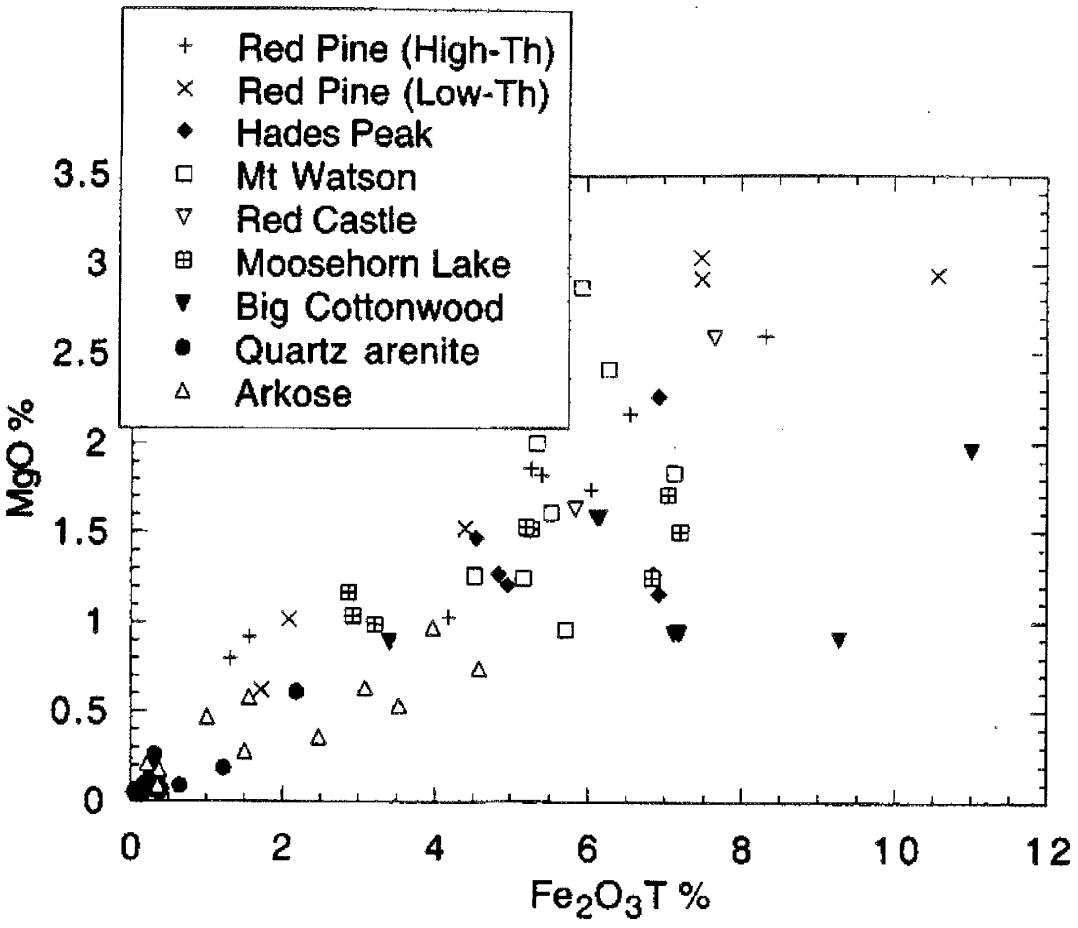

Fig. 10: MgO-Fe_2O_3T graph showing the distribution of sediments from the Uinta Mountain and Big Cottonwood groups. All samples with formation names are shales and siltstones.

As expected, quartz arenites have very little Mg and Fe. Arkoses, however, which contain variable amounts of biotite and chlorite, have intermediate Fe and Mg contents.

On a plot of the Chemical Index of Alteration (CIA Index; Nesbitt and Young, 1982) versus the Al_2O_3/TiO_2 ratio, Uinta Mountain and Big Cottonwood shales and sandstones define two distinct trends (Fig. 11). As expected, shales have high CIA indices (mostly 75-85) reflecting significant chemical weathering of their sources. They fall in a tight group showing a slight increase in Al_2O_3/TiO_2 ratio with increasing CIA, suggesting a somewhat greater residual nature of Al_2O_3 compared to TiO_2. In contrast, Uinta Mountain Group sandstones exhibit a broad inverse correlation between the CIA and Al_2O_3/TiO_2 values (Fig. 11). Quartz arenites are scattered reflecting sensitivity to small differences in modal Fe-Ti oxides as well as possible diagenetic remobilization of alkalies (affecting the CIA index). The spread in Al_2O_3/TiO_2 values in the sandstones chiefly reflects variation in the feldspar/quartz ratio and thus, is a measure of sandstone maturity. The three quartz arenites that plot with arkoses in Figure 11 are sericite quartz arenites and the high Al_2O_3/TiO_2 ratio reflects the sericite content of these samples.

With regard to major elements, no apparent relationship exists between chemical composition and either stratigraphic level or geographic location in the western Uinta Mountain Group or in the Big Cottonwood Group.

Trace Elements

As first recognized by Ball and Farmer (1998), the most unusual feature of many of Uinta Mountain Group shales is their relatively high Th contents. Some Uinta Mountain Group shales contain > 40 ppm Th, considerably higher than most Phanerozoic shales,

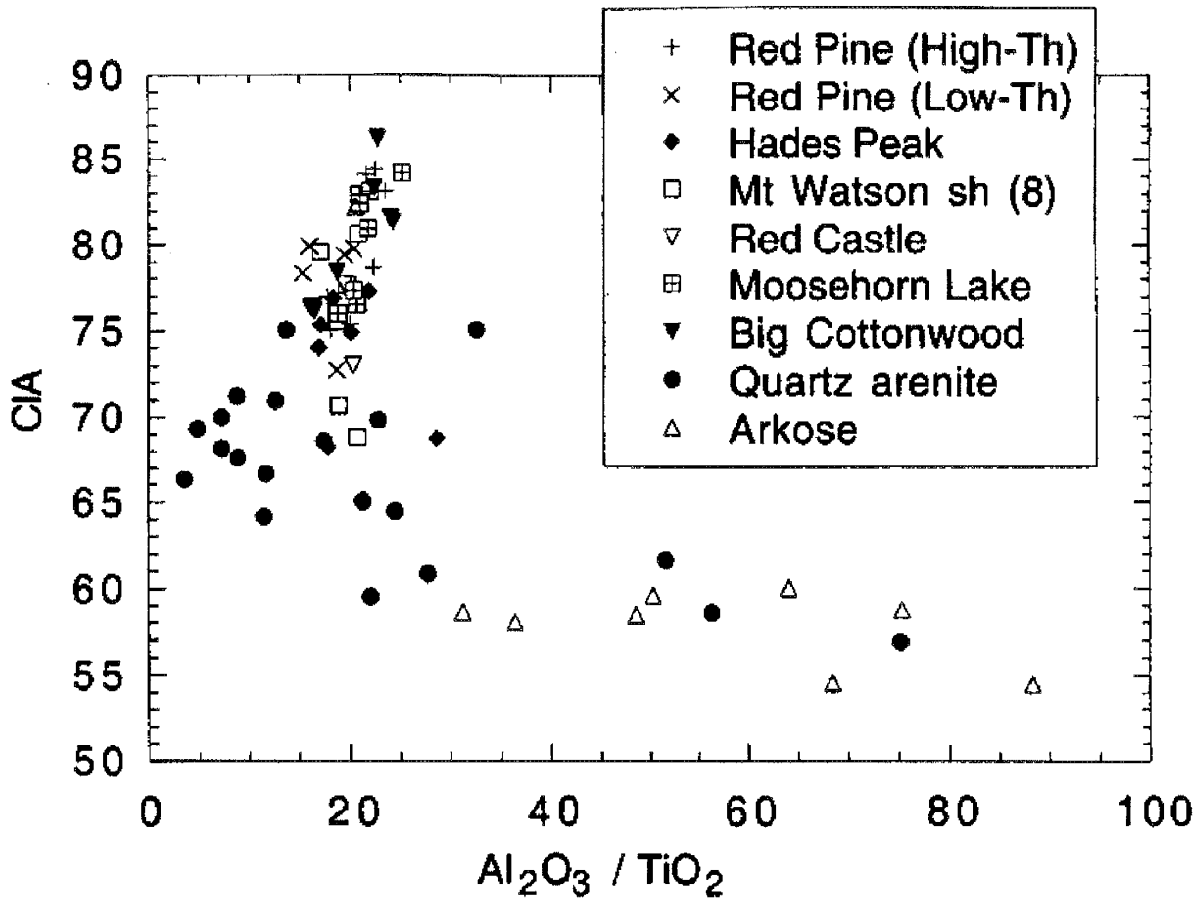

Fig. 11: Chemical Index of Alteration (CIA) versus Al_2O_3/TiO_2 graph showing the distribution of sediments from the Uinta Mountain and Big Cottonwood groups. CIA = $Al_2O_3/ Al_2O_3 + CaO + Na_2O + K_2O$, molecular ratio, where CaO is silicate fraction only (Nesbitt et al., 1997). All samples with formation names are shales and siltstones.

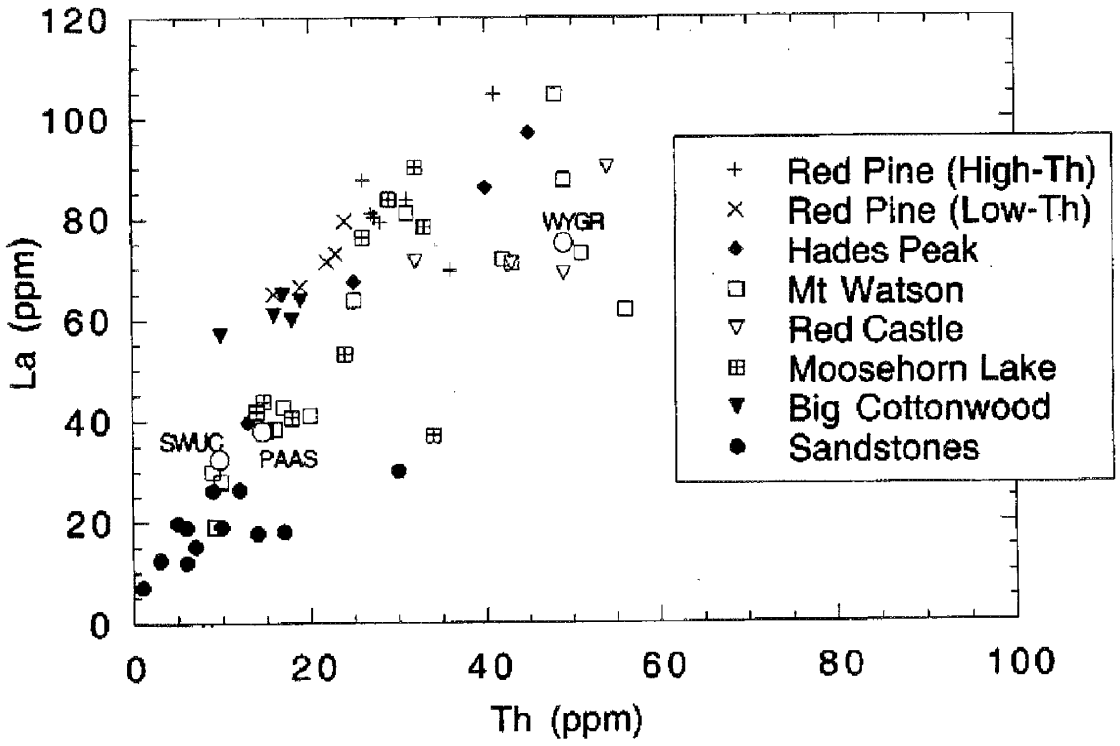

Fig. 12: La – Th graph showing the distribution of sediments from the Uinta Mountain and Big Cottonwood groups. SWUC, average composition of Paleoproterozoic upper crust from the southwestern United States (Condie and Chomiak, 1996); WYGR, average composition of Archean granites from the Wyoming craton (data from Rosholt, 1983; Stuckless, 1989). PAAS, Proterozoic Average Australian Shale (Taylor and McLennan, 1985). All samples with formation names are shales and siltstones.

which are generally < 20 ppm Th (Fig. 12) (Condie, 1993). Broadly correlated with Th in Uinta Mountain Group shales are U, REE, Y, Zr, and Hf, which are also relatively high in many of the shales (Fig. 12). This study refers to shales with > 25 ppm Th as high-Th types and those with ≤ 25 ppm as low-Th types. There is a continuum between the two shale types with the highest Th contents in shales of the Red Pine, Mt. Watson, Red Castle, and Hades Peak Formations. With exception of the Big Cottonwood Group and Moosehorn Lake Formation, which contain only low-Th shales, both high- and low-Th shales occur in all of the formations. Th and U are distinct in some shales where they are enriched more than REE, Y, Zr, and Hf. In general, both low- and high-Th shales are enriched by about a factor of two in most elements compared to average Archean upper crust, whereas Th and U in high-Th shales are enriched by a factor of three or more (Fig. 12). In contrast to shales, Uinta Mountain Group quartz arenites and arkoses typically have low contents of Th (mostly < 20 ppm), REE, Y, Zr, and Hf.

Shales of the Uinta Mountain Group have chondrite-normalized light-REE (LREE) enriched patterns with negative Eu anomalies and gently sloping heavy-REE (HREE) (Fig. 12). Eu/Eu* values range from about 0.5 to 0.65, typical of most Phanerozoic shales. LREE are enriched in most of the Uinta Mountain and Big Cottonwood shales to a greater degree than in most shales of all ages (Fig. 13) (Condie, 1991; 1993). Only the Mt. Watson, Hades Peak, and Moosehorn Lake Formations contain some shales with "normal" LREE contents. Because Uinta Mountain Group shales do not appear to contain minor phases like allanite or monazite, which are highly enriched in LREE (Gromet and Silver, 1983), the peculiar LREE-enriched character of most of these rocks was probably inherited from their sources. REE patterns in Uinta Mountain Group

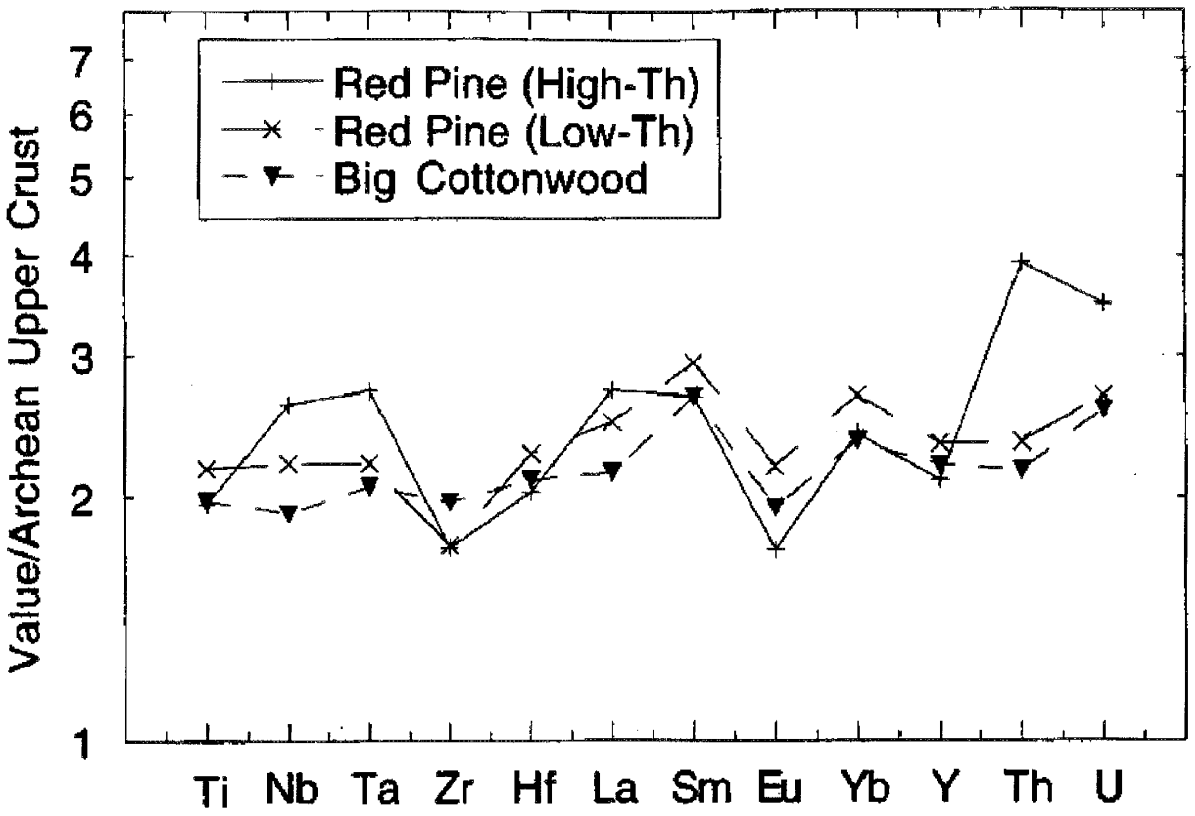

Fig. 13: Distribution of high field strength elements and REE in sediments from the Uinta Mountain and Big Cottonwood Groups. Data are normalized to average Archean upper crust from Condie (1993).

quartz arenites and arkoses are variable, although many show patterns typical of shales suggesting a predominant clay/mica control (with quartz dilution) (Fig. 15). Similar results are reported for quartz arenites of the Paleoproterozoic Snowy Pass Supergroup in southeast Wyoming (Crichton and Condie, 1993). The fact that all of the Uinta Mountain Group arkoses have negative Eu anomalies indicates that feldspar accumulation in these sediments has not offset Eu anomalies inherited from the source rocks (although it may have decreased the size of the Eu anomaly).

Overall positive correlations of REE, Y, Zr, and Hf with Al_2O_3 in Uinta Mountain and Big Cottonwood shales suggests that these elements are mainly housed in clays and micas. Because HREE are not correlated with Zr or Hf, and $(Gd/Yb)_n$ ratios are low (< 2) (Fig. 16), it is unlikely that zircon is an important HREE-bearing phase in the shales. Similar findings are reported for Phanerozoic shales (Condie, 1991). Variable and crossing chondrite-normalized HREE patterns in Uinta Mountain Group quartz arenites and arkoses (for example MW-2 and RC-9), however, suggest that HREE distributions in these rocks may be controlled by minor minerals (Fig. 16). An overall positive correlation of Zr (and Hf) with Yb in Uinta Mountain Group sandstones suggests that HREE in these rocks are at least in part controlled by detrital zircon. This cannot be the entire story, however, since LREE correlate with Al_2O_3 in the sandstones and $[Gd/Yb]_n$ ratios are typically much greater than those found in zircon. It would appear that clay/mica chiefly control the light and intermediate REE, whereas zircon chiefly controls the heavy REE in the sandstones.

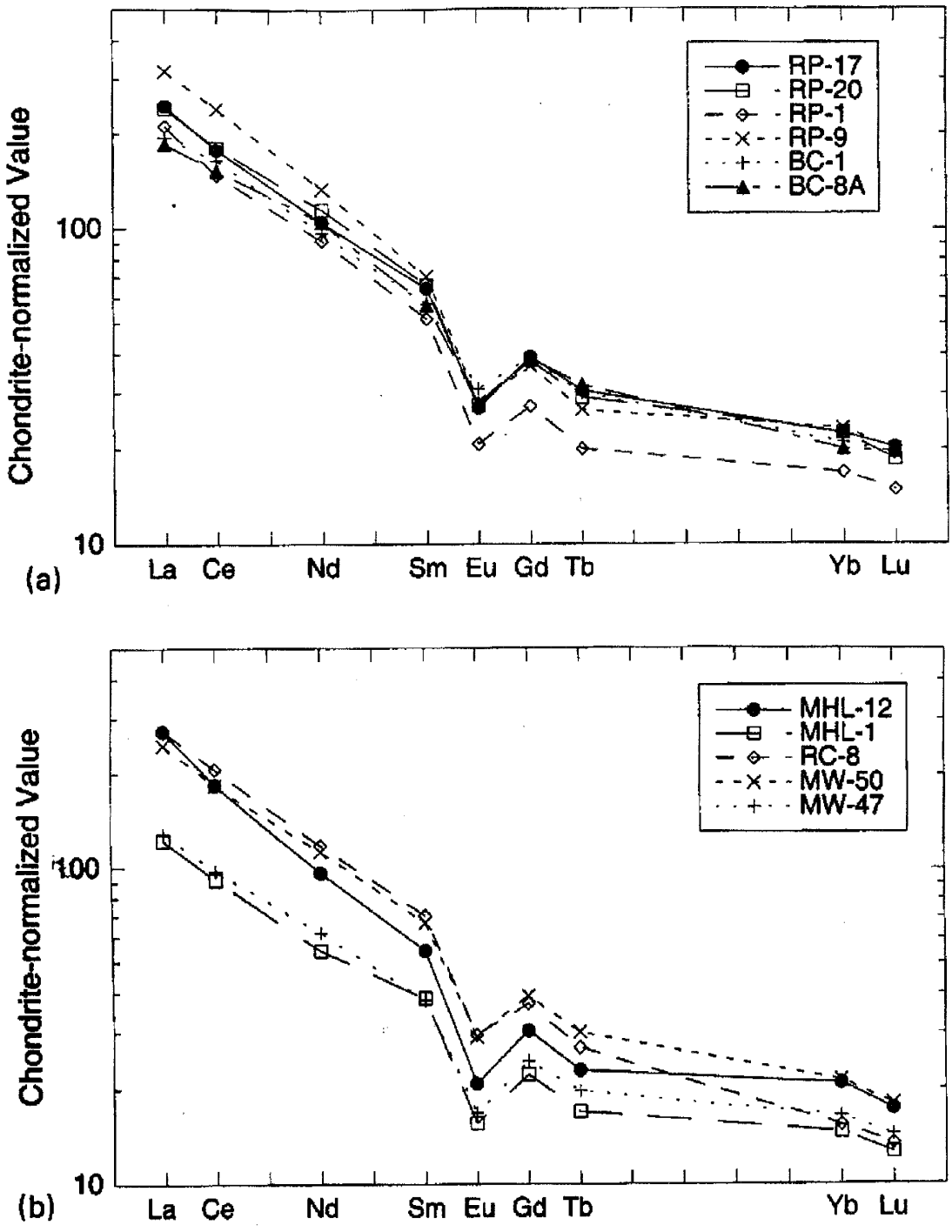

Fig. 14: Chondrite-normalized REE distributions in shales from the Uinta Mountain and Big Cottonwood groups. a) Big Cottonwood Group and Red Pine Shale; b) Moosehorn Lake, Red Castle, and Mt. Watson Formations. Chondrite values from Haskin et al. (1968).

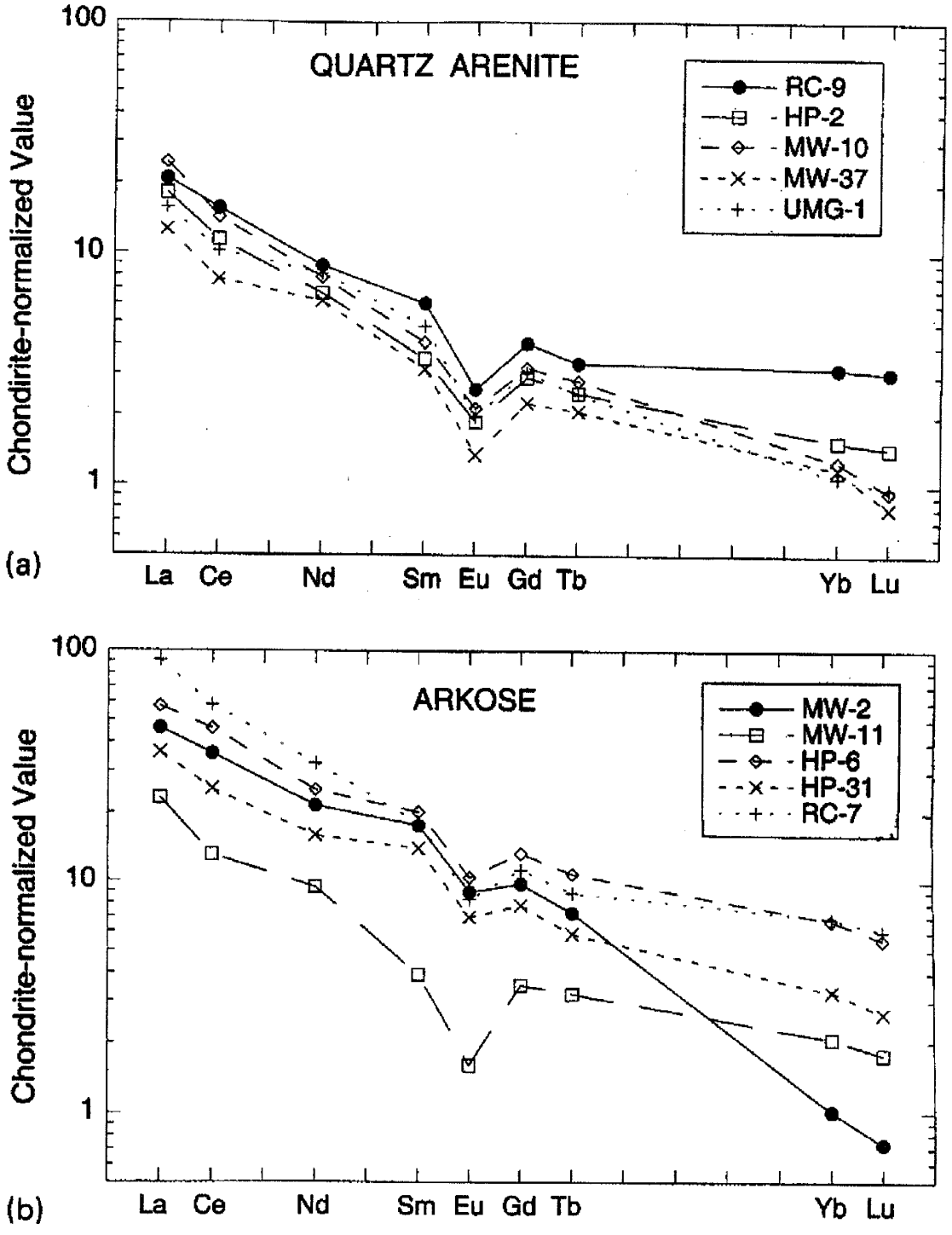

Fig. 15: Chondrite-normalized REE distributions in a) quartz arenite and b) arkose from the Uinta Mountain Group. Chondrite values from Haskin et al. (1968).

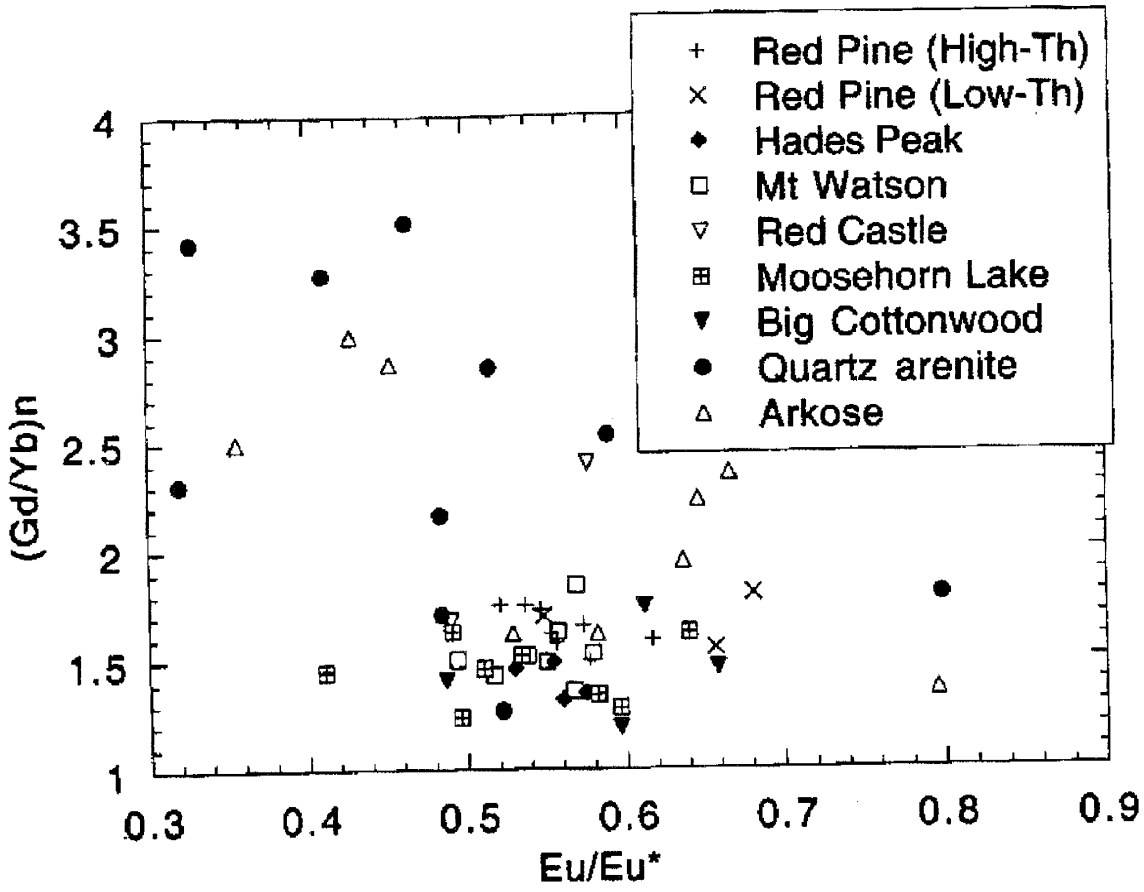

Fig. 16: (Gd/Yb)n versus Eu/Eu* graph showing the distribution of sediments from the Uinta Mountain and Big Cottonwood Groups. (Gd/Yb)n, ratio normalized to average chondritic meteorites (Haskin et al.,1968). All samples with formation names are shales and siltstones.

Discussion

Tectonic Setting

Although previous studies have suggested a rift or aulacogen tectonic setting for the Uinta Mountain Group (Ball and Farmer, 1998), the problem of how to account for a mixture of immature arkose and mature quartz arenite in the same succession has not been adequately addressed. Detrital mode studies confirm the presence of both of these types of sandstone in the western part of the Uinta Mountain basin (Fig. 8). In the Big Cottonwood Group, however, arkose has not been found in this study or by previous investigators (Chan et al., 1994; Ehlers et al., 1997). On the Dickinson detrital mode graph, as well as on most major element diagrams (Figs. 8-11), the two sandstone populations are well-defined. On the Dickinson plot, quartz arenites plot in the craton interior or transition field and arkoses plot in the transition or basement uplift field (Fig. 8). Taken at face value, this suggests variable tectonic settings in the Uinta Mountain Group, which is not possible since both types of sandstone are interbedded. If the Uinta Mountain Group was deposited in a rift basin as seems likely (see below), where do the pure quartz sands come from? As suggested by earlier studies and by this study's paleocurrent data (Sanderson, 1984), it would appear that in the western Uinta Mountain basin, arkose came dominantly from the Archean Wyoming craton to the north, whereas quartz arenite was derived from more eastern sources, perhaps transported great distances by a major drainage system as suggested by Ball and Farmer (1998). This emphasizes the fact that detrital modes alone may not be sufficient

to identify ancient tectonic settings, because sandstones with the mineralogical characteristics of one tectonic setting may under some circumstances be deposited in another tectonic setting.

Paleoweathering Conditions

The Chemical Index of Alteration (CIA index) as well as the A-CN-K triangular graph are widely used to constrain paleoweathering conditions of ancient shales (Fig. 17)(Nesbitt and Young, 1982; Fedo et al., 1995; Nesbitt et al., 1997). A potential problem in using geochemical indices to constrain paleoclimates is that of recycling of previously weathered detritus. Although we cannot quantitatively evaluate the recycling effect for the Uinta Mountain and Big Cottonwood groups, there are several lines of evidence that suggest it was minimal:

1. Shale is a very minor component within Paleoproterozoic and Archean successions in the Rocky Mountain region, and hence shale recycling should be minor (Condie, 1992).
2. The K_2O/Al_2O_3, Zr/Sc and Th/Sc ratios, which are high in extensively recycled sediments (McLennan et al., 1993; Cox et al., 1995), are not high in the Uinta Mountain or Big Cottonwood shales.
3. Textures of arkose and feldspathic quartz arenite closely associated with shales are typically immature and many of these sandstones contain relatively fresh detrital feldspars. Conglomerates contain clasts of vein quartz, chert, and various granitoids.

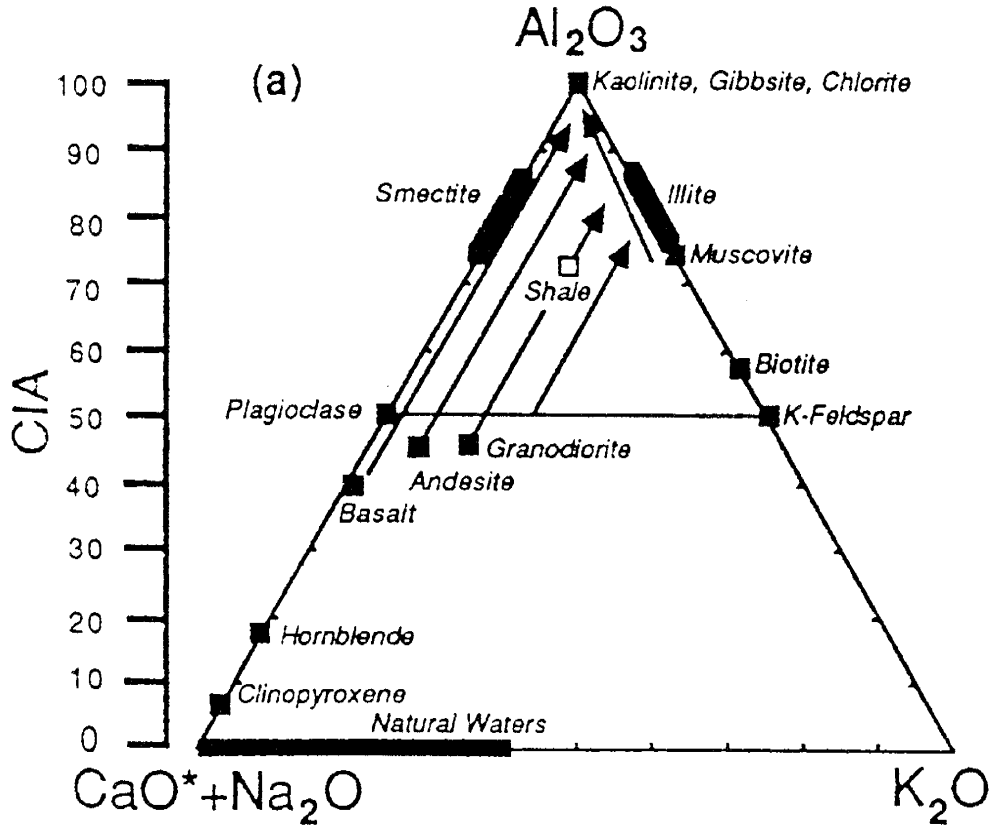

$$CIA = 100 \times [Al_2O_3/(Al_2O_3 + CaO^* + Na_2O + K_2O)]$$

or

$$CIA = 100 \times [A/(A + C + N + K)]$$

Fig. 17: A-CN-K plot showing the distribution of weathering trends from Nesbitt et al. (1997).

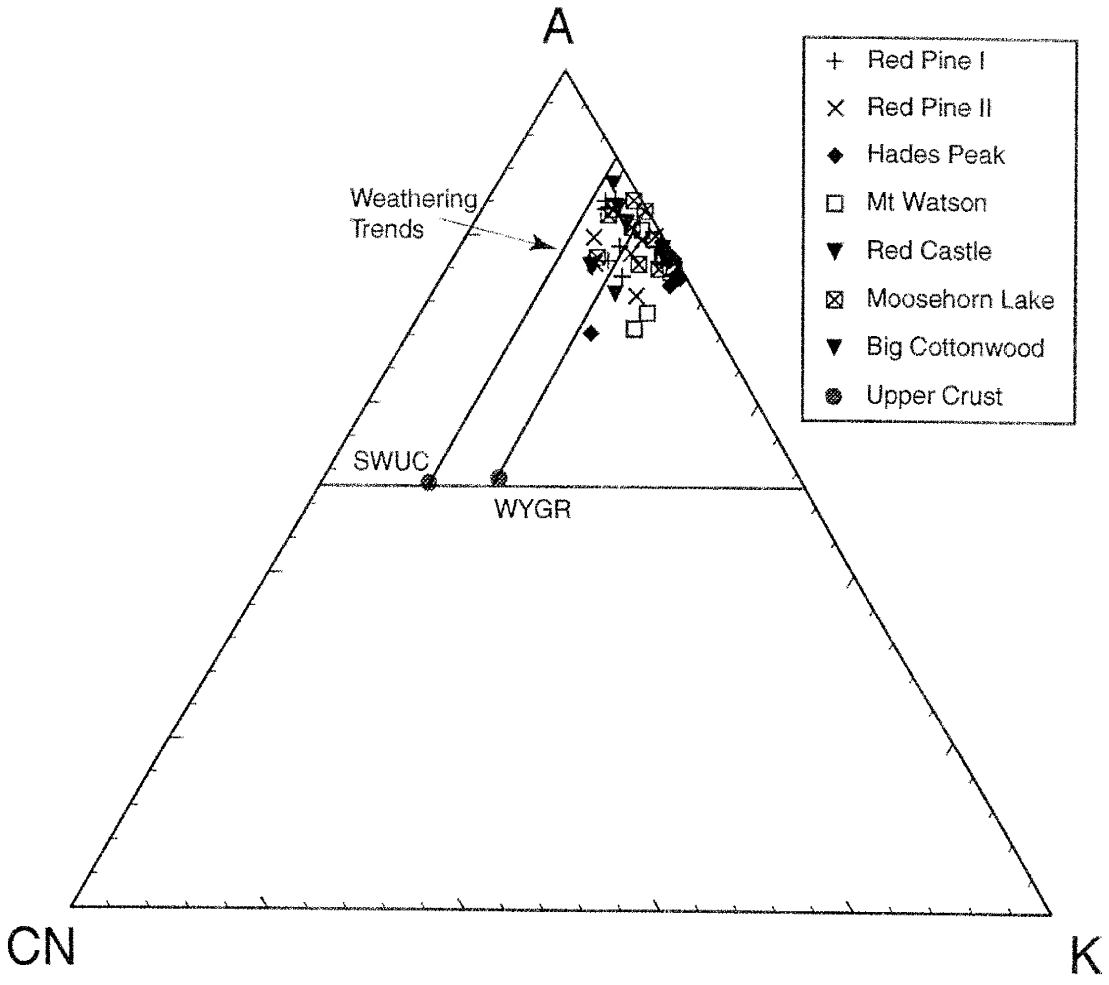

Fig. 18: A-CN-K plot showing the distribution of shales from the Uinta Mountain and Big Cottonwood groups. Weathering trends from Nesbitt et al. (1997).

4. Other than chert, which probably comes from Archean and Proterozoic greenstones in the basement, few sedimentary rock fragments are present in the Uinta Mountain Group sandstones.

For these reasons, this study suggests that the A-CN-K chemical relationships portrayed by the Uinta Mountain and Big Cottonwood shales can be useful in constraining the paleoweathering conditions in the sediment sources.

Most of these Neoproterozoic shales plot on or close to the AK join and at high A values in the A-CN-K system (Fig. 18). The fact that shales do not lie on a line projecting back to a probable source, as is the case in some studies (Fig. 17) (Fedo et al., 1995; Nesbitt et al., 1997), appears to result from a combination of two factors. First, as discussed below, it would appear that these sediments were derived from both Paleoproterozoic upper crust and Archean upper crust, the latter of which contained a large proportion of Th-enriched granites. Approximately half of the shales fall in the field bracketed by weathering trends emanating from average Paleoproterozoic upper crust of Southwest Laurentia (SWUC) and average granite from the Wyoming craton (WYGR), thus accounting for the spread of shale compositions as a source effect. A second cause may be K-metasomatism. Some of the shales fall on the K-rich side of the field bracketed by the weathering trends, possibly supporting K-enrichment during diagenesis (Fedo et al., 1995). The shales most affected by K-metasomatism are those from the Hades Peak, Red Castle, and Mt. Watson Formations. Despite the effects of variable source composition and K-metasomatism, the tight grouping of the Uinta Mountain and Big Cottonwood shales and the relatively high A values and high CIA

indices (Figs. 11 and 18) suggest a high degree of weathering in the sediment sources. This is interpreted to reflect steady state weathering probably under tropical to subtropical conditions (Nesbitt et al., 1997). Such conditions are consistent with the probable low-latitude location of this part of Laurentia 800 Ma just as the supercontinent Rodinia began to fragment (Powell et al., 1994; Dalziel, 1997).

Provenance

Previous field and sedimentologic studies as well as Nd isotopic studies of the Uinta Mountain Group suggest mixed provenance with arkose coming chiefly from the Wyoming craton to the north and quartz arenite derived from more eastern sources including both Archean and Paleoproterozoic input (Ball and Farmer, 1998). New Nd isotopic data support this idea (Condie, et al, 2001). Most of the high-Th shales in the Uinta Mountain Group, as well as the few sandstones that have been analyzed (Ball and Farmer, 1998), have measured ε_{Nd} values (-22 to –28) and $^{147}Sm/^{144}Nd$ ratios that suggest they come chiefly from the Wyoming craton (Fig. 20). In contrast, low-Th shales in studies by Condie, et al. (2001) and Ball and Farmer (1998), have higher measured ε_{Nd} (-20 to –23) and may represent mixtures of Archean and ~1.8-Ga upper crustal provenance or sediments derived from Paleoproterozoic crustal sources with "mixed" Archean and Proterozoic Nd isotopic characteristics (i. e., "Province 1"; Fig. 13) (Bennett and DePaolo, 1987).

Cr/Th and Th/Sc ratios are particularly sensitive to the composition of shale sources (Taylor and McLennan, 1985; Condie and Wronkiewicz, 1990). On a plot of these two

ratios, the Uinta Mountain and Big Cottonwood shales define a smooth curve suggestive of mixing (Fig. 19). The average composition of Paleoproterozoic upper crust in the Southwestern United States plots near the high Cr/Th end of this curve and the average composition of Archean granite from the Wyoming craton falls near the high Th/Sc end. The average granite composition includes chiefly data from Archean granites exposed in central Wyoming (Stuckless et al., 1977; Rosholt, 1983; Stuckless, 1989). It is noteworthy that these granites are unusual compared to most Archean granites in that they are variably enriched in Th and U, and in some cases in LREE. This again emphasizes the fact that the Archean Wyoming craton is unusual compared to most other Archean cratons in being enriched in Th, U, and radiogenic Pb (Wooden and Mueller, 1988; Frost et al., 1998).

Generally, the Uinta Mountain and Big Cottonwood shales can be explained by mixing of the SWUC and WYGR end members using the Cr/Th-Th/Sc and the La-Th diagrams (Figs. 12 & 19). The shales from the Big Cottonwood Group and the low-Th Red Pine suite fall near the SWUC end member suggesting no direct contribution of Archean granite into these sediments. This indicates that little if any Archean source material was transported westward into the Big Cottonwood basin and that some of the Red Pine shales were derived exclusively from low-Th sources. As determined in Condie, et al. (2001), low-Th shales have relatively hi Σ_{Nd} values in this study area.

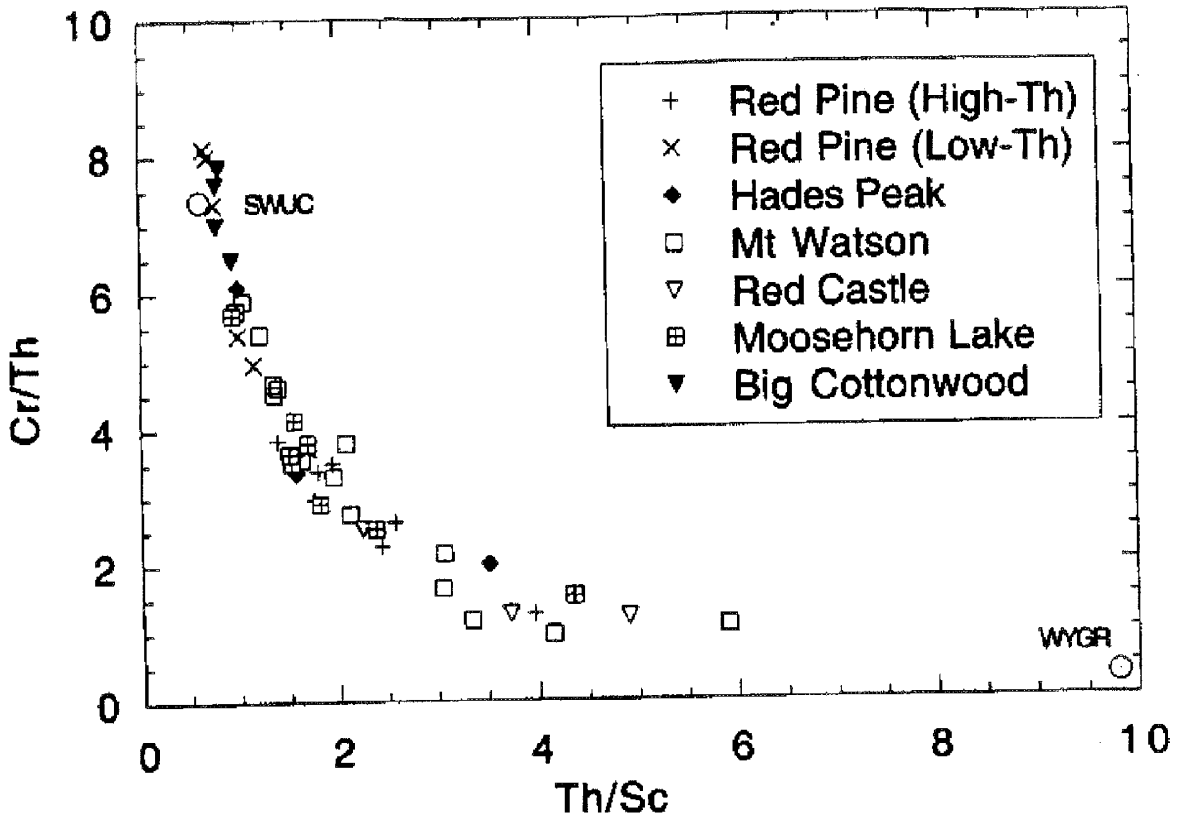

Fig. 19: Cr/Th – Th/Sc graph showing the distribution of shales from the Uinta Mountain and Big Cottonwood groups. .

Because low-Th shales have relatively high ε_{Nd} values and high-Th shales have low ε_{Nd} values, it would appear that shales from these two groups were derived chiefly or exclusively from Paleoproterozoic sources. In contrast, many of the high-Th shales from the Mt. Watson and Red Castle Formations have a large contribution from granite-rich Archean sources. The relative enrichment in REE (especially LREE), Y, Zr, and Hf in some shales may have been inherited from Archean granites anomalously enriched in these elements.

Collectively, field, petrographic, and Nd and trace element results support a mixed provenance for the Uinta Mountain Group, with arkoses being derived dominantly from the Wyoming craton, quartz arenite from mixed Archean and Paleoproterozoic sources to the east, and shale from both sources (Fig. 20). The Nd isotopic characteristics of the Big Cottonwood Group are identical to those of low-Th shales in the Uinta Mountain Group requiring a " Nd Province 1" or mixed Archean and Paleoproterozoic provenance.

Because the Wyoming craton contains greenstones and TTG (tonalite-trondhjemite-granodiorite) complexes (Frost and Frost, 1993), the lack of evidence for these source rocks in the Uinta Mountain Group sedimentary rocks may be important in terms of uplift history of the Wyoming craton. The greenstone-TTG complexes generally occur at shallow levels in Archean cratons and should be eroded first. Does this mean the Wyoming craton had a history of uplift and erosion prior to deposition of the Uinta Mountain Group in which the greenstone-TTG component was largely removed? Perhaps most of this component ended up in the Snowy Pass Supergroup or other Paleoproterozoic successions around the perimeter of the craton (Crichton and Condie, 1993). By the time the Uinta Mountain Group rift formed in the Neoproterozoic,

previous erosion had exposed high-Th granites which became the primary source for much of the Uinta Mountain Group sediments. The Big Cottonwood Group depocenter, however, lay to the west outside of the rift and received relatively minor amounts of sediment from the Archean craton. The main source of the Big Cottonwood Group sediments appears to have been a westward-flowing river system in the Uinta Mountain Group rift basin (Fig. 20), a possibility supported by the fact that Uinta Mountain Group sediments deposited from this river system and the Big Cottonwood Group sediments have identical Nd isotopic compositions.

Paleogeography

Some investigators have suggested that the Uinta Mountain Group was deposited in an east-trending aulacogen that opened to the west into a deep ocean (Sears et al., 1982). But this study would indicate that the Uinta Mountain Group basin probably opened into a shallow seaway on the west in the Neoproterozoic, and that it was not an aulacogen. Aulacogens, which form during the breakup of supercontinents, open into new ocean basins like many of those around the Atlantic Ocean today. Because Neoproterozoic sediments rest on older Proterozoic and Archean basement as far west as northeastern Nevada (Link et al., 1993), oceanic crust did not exist in this area in the Neoproterozoic (Fig. 20). There was at least 500 km between the western end of the Uinta Mountain rift and the edge of the continental shelf, and thus the rift terminated within, rather than at the edge of the craton, as it should if it were an aulacogen. When Rodinia began to break up at about the time the Uinta Mountain and Big Cottonwood

groups were deposited, the rifted continental margin may have been somewhere in west-central Nevada. This research favors an intracratonic rift for deposition of the Uinta Mountain Group. This rift probably contained a major river system flowing from the east, perhaps coming from as far as South Dakota (Ball and Farmer, 1998). The absence of igneous rocks in the Uinta Mountain Group argues against a mantle plume origin for the Uinta Mountain rift, and in this respect it differs from the 1-Ga Mid-Continent rift where mafic igneous rocks are abundant. The stresses that produced the Uinta Mountain Group rift may have been related to initial rifting of Antarctica or Australia from the Laurentia beginning about 800 Ma (Fig. 1).

Because the Uinta Mountain Group arkosic sediment entered the rift basin from the north and northeast, it would appear that the rift basin was asymmetric, with an active normal fault system on the north, with little sediment coming from southern sources (Fig. 3, 20). Sedimentary environments ranged from intertidal estuarine types in the Big Cottonwood depocenter on the west, extending into the extreme western part of the Uinta Mountain Group rift, to fluvial in most of the rift. Much of the Uinta Mountain Group appears to have been deposited in a braided stream system (Sanderson, 1984). Paleoproterozoic sources were either in Colorado or further to the east. The well-rounded quartz sand in some of the quartz arenites in the western part of the Uinta Mountain Group basin is not commonly produced in fluvial environments. One possible source for this sand is eolian dune fields along the southern margin of the Uinta Mountain Group rift. The dune sands may have been reworked by fluvial systems and redeposited along the Uinta Mountain Group rift by a major river system flowing along its axis (Ball and Farmer, 1998).

It is also noted that at least some Neoproterozoic detrital sediments deposited in a shelf environment along the Nevada-Utah state line (Trout Creek and McCoy Creek Groups in westernmost Utah and NE Nevada) have Nd isotopic compositions significantly different from those of the Big Cottonwood Group (Condie, et al, 2001). This isotopic contrast suggests that the river system responsible for deposition of the Uinta Mountain and Big Cottonwood groups was not the source of all shallow marine sediments deposited west of the Big Cottonwood depocenter. Instead, the Trout Creek Group is interpreted to represent detritus eroded from local Paleoproterozoic basement rocks uplifted along the southern rift flank of the Uinta Mountain basin (Nd Provinces 2 and 3) (Farmer and Ball, 1997). If the Big Cottonwood Group is older than the Trout Creek Group (Link et al., 1993), this implies the development of an uplift (the proto Toole-Uinta arch?) that blocked the westward flow of the Uinta Mountain Group river system and prevented delivery of sediments with Nd Province 1 sources to this portion of the newly formed continental margin of Laurentia (Fig. 20). However, the Neoproterozoic McCoy Creek Group, which overlies the Trout Creek Group in easternmost Nevada and western Utah, has similar Nd isotopic characteristics to the Big Cottonwood Group (Condie, et al, 2001). Farmer and Ball (1997) interpreted the McCoy Creek Group as having been derived from an east-west anticline, cored in Paleoproterozoic basement (Nd Province 1), again possibly the proto Toole-Uinta arch (Fig. 20). In light of the new data from the Big Cottonwood Group herein reported, it is also possible that the Neoproterozoic shallow marine sediments that are interpreted to have been derived from Nd Province-1 were derived from reworked equivalents of the Big Cottonwood Group. Alternatively, they may represent sediments transported across

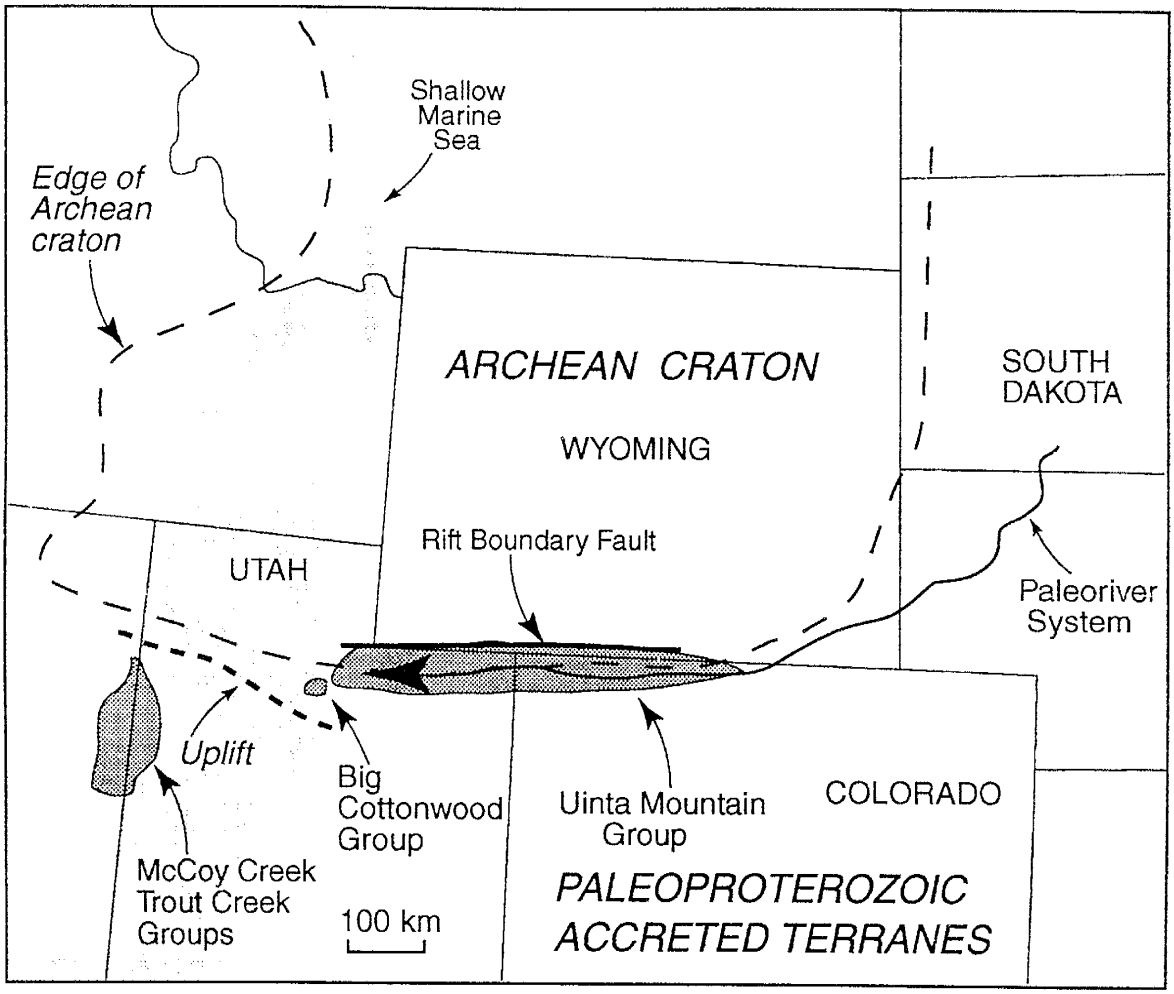

Fig. 20: Generalized tectonic map showing possible paleogeographic reconstruction of the Uinta Mountain and Big Cottonwood depositional systems about 800 Ma. Suture between the Archean Wyoming craton and Paleoproterozoic terranes coincides with the southern edge of the Wyoming craton. Small arrows indicate paleocurrent directions inferred from cross-bedding (Sanderson, 1984).

the region south of the Uinta Mountain Group basin from the distal portions of the continent by an east-west oriented drainage system similar to that recorded by the Uinta Mountain Group. However, because there is no Nd isotopic evidence for Grenvillian sources (1.3-1.0 Ga), such a drainage could not come from great distances to the south or southeast where Grenville rocks occur.

Conclusions

1. The Neoproterozoic Uinta Mountain Group appears to have been deposited in an east-trending intracratonic rift bounded along the north by an active fault system and opening into a shallow sea to the west where the Big Cottonwood Group was deposited. Although this rift may have been associated with the early stages in the breakup of Rodinia, it was not an aulacogen.
2. Uinta Mountain Group sediments were derived from mixed Archean and Paleoproterozoic sources with the former dominating, whereas Big Cottonwood Group sediments appear to be derived chiefly from Paleoproterozoic sources.
3. The Archean sediment source is the Wyoming craton on the north side of the rift basin, and source rocks were dominated by granites enriched in Th, U, Y, Zr, Hf, and REE. The relative abundance of enriched granite in the Archean Wyoming craton implied by the Uinta Mountain sediments indicates the Wyoming craton is anomalous compared to other Archean cratons.
4. CIA values and A-CN-K relationships in shales of the Uinta Mountain and Big Cottonwood groups indicate significant weathering of sources, probably in subtropical to tropical climates supporting a near-equatorial location for southwestern Laurentia c. 800 Ma.

References

Ball, T. T. and Farmer, G. L., 1998. Infilling history of a Neoproterozoic intracratonic basin: Nd isotope provenance studies of the Uinta Mountain Group, western United States. Precamb. Res., 87: 1-18.

Bennett, V. C., and DePaolo, D.J., 1987. Proterozoic crustal history of the western United States as determined by neodymium isotopic mapping. Geol. Soc. America Bull., 99: 674-685.

Chan, M. A., Kvale, E. P., Archer, A. W., and Sonett, C. P., 1994. Oldest direct evidence of lunar-solar tidal forcing encoded in sedimentary rhythmites, Proterozoic Big Cottonwood Formation, central Utah. Geology, 22: 791-794.

Condie, K.C., 1991. Another look at REE in shales, Geochim. Cosmochim. Acta, v. 55, p. 2527-2532.

Condie, K.C., 1992. Proterozoic terranes and continental accretion in southwestern North America. In: K.C. Condie (Editor), Proterozoic Crustal Evolution, Elsevier Scient. Publishers, Amsterdam, Chapt. 12, p. 447-480.

Condie, K.C., 1993. Chemical composition and evolution of the upper continental crust: contrasting results from surface samples and shales, Chemical Geology, v. 104, p. 1-37.

Condie, K.C. and Wronkiewicz, D.J., 1990. The Cr/ Th ratio in Precambrian pelites from the Kaapvaal Craton as an index of craton evolution. Earth Planet. Sci. Lettr., 97: 256-267.

Condie, K. C. and Chomiak, Beverly, 1996. Continental accretion: contrasting Mesozoic and Early Proterozoic tectonic regimes in North America. Tectonophysics, v. 265: 101-126.

Condie, K. C., Farmer, G. Lang, and Lee, Dennis, 2001. Tectonic setting and provenance of the Uinta Mountain and Big Cottonwood groups, northern Utah: constraints from geochemistry, Nd isotopes, and detrital modes. Sedimentary Geology, v. 141-142: 443-464.

Cox, R., Lowe, D. R. and Cullers, R. L., 1995. The influence of sediment recycling and basement composition on evolution of mudrock chemistry in the SW US. Geochim. Cosmochim. Acta, 59: 2919-2940.

Crichton, J.G. and Condie, K.C., 1993. Trace elements as source indicators in cratonic sediments: A case study from the Early Proterozoic Libby Creek Group, Southeastern Wyoming, Journal of Geology, v. 101, p. 319-332.

Dalziel, I. W., 1997. Neoproterozoic-Paleozoic geography and tectonics: review, hypothesis, environmental speculation. Geol. Soc. Amer. Bull., 109: 16-42.

Dickinson, W. R. et. al., 1983. Provenance of North American Phanerozoic sandstones in relation to tectonic setting. Geol. Soc. Amer., Bull., 94: 222-235.

Ehlers, T. A., Chan, M. A., and Link, P. K., 1997. Proterozoic tidal, glacial, and fluvial sedimentation in Big Cottonwood Canyon, UT. Brigham Young Univ., Geology Studies, 23: 31-58.

Ehlers, T. A. and Chan, M. A., 1999. Tidal sedimentology and estuarine deposition of the Proterozoic Big Cottonwood Formation, Utah. J. Sed. Res., 69: 1169-1180.

Farmer, G.L. and DePaolo, D. J., 1983. Origin of Mesozoic and Tertiary granite in the western United States and implications for pre-Mesozoic crustal structure 1. Nd and Sr isotopic studies in the geocline of the northern Great Basin. J. Geophys. Res., 88: 3379-3401.

Farmer, G. L., Broxton, D. E., Warren, R. G., and Pickthorn, W., 1991. Nd, Sr, and O isotopic variations in metaluminous ash-flow tuffs and related volcanic rocks at the Timber Mountain/Oasis Valley Caldera Complex, SW, Nevada: implications for the origin and evolution of large-volume silicic magma bodies. Contrib. Mineral. Petrol.,109: 53-68.

Farmer, G. L. and Ball, T. T., 1997. Sources of Middle Proterozoic to Early Cambrian siliciclastic sedimentary rocks in the Great Basin: a Nd isotope study. Geol. Soc. Amer., Bull., 109: 1193-1205.

Fedo, C. M., Nesbitt, H. W. and Young, G. M., 1995. Unraveling the effects of potassium metasomatism in sedimentary rocks and paleosols, with implications for paleoweathering conditions and provenance. Geology, 23: 921-924.

Frost, C. D. and Frost, B. R., 1993. The Archean history of the Wyoming province. In: Snoke, S. W., Steidtmann, J. R., and Roberts, S. M. (Eds.), Geology of Wyoming. Geol. Soc. Wyoming, Mem. 5: 58-76.

Frost, C. D., Frost, B. R., Chamberlain, K. R., and Hulsebosch, T. P., 1998. The Late Archean history of the Wyoming province as recorded by granitic magmatism in the Wind River Range, Wyoming. Precamb. Res., 89: 145-173.

Gromet, L. P. and Silver, L. T., 1983. Rare earth element distributions among minerals in a granodiorite and their petrogenetic implications. Geochim. Cosmochim. Acta, 47: 925-939.

Hallett, B. R. and Kyle, P. R.,1993. XRF and INAA determinations of major and trace elements in Geological Survey of Japan igneous and sedimentary rock standards. Geostandards Newslett., 17(1): 127-133.

Haskin, L. A., Haskin, M. A., Frey, F. A., and Wildeman, T. R.,1968. Relative and absolute terrestrial abundances of the REE. In Origin and Distribution of the Elements. pp. 889-912, Pergamon Press, NY.

Helmold, K. P., 1985. Provenance of feldspathic sandstones-the effect of diagenesis on provenance interpretations: a review. In: G. G. Zuffa (Ed.), Provenance of Arenites. Reidel, p. 139-163.

James, L. P., 1979. Geology, ore deposits, and history of the Big Cottonwood mining district,, Salt Lake County, Utah. Utah Geol. Mineral. Surv. Bull., 114, 90 p.

Link, P. K., et al., 1993. Middle and Late Proterozoic stratified rocks of the western US Cordillera, Colorado Plateau, and Basin and Range Province. Geol. Soc. Amer., Geology of North America, vol. C-2: 463-596.

McDaniel, D. K. et al., 1994. Resetting of Nd isotopes and redistribution of REEs during sedimentary processes: the Early Proterozoic Chemsford Fm, Sudbury basin, Ontario, Canada. Geochim. Cosmochim. Acta, 58: 931-941.

McLennan, S. M., Hemming, S., McDaniel, D. K., and Hanso, G. N., 1993. Geochemical approaches to sedimentation, provenance, and tectonics. Geol. Soc. America, Sp. Paper 284: 21-40.

Milliken, K. L., 1988. Loss of provenance information through subsurface diagenesis in Plio-Pleistocene sandstones, N Gulf of Mexico. J. Sed. Petrol., 58: 992-1002.

Nesbitt, H. W. and Young, G. M., 1996. Petrogenesis of sediments in the absence of chemical weathering: effects of abrasion and sorting on bulk composition and mineralogy. Sedimentol., 43: 341-358.

Nesbitt, H. W., Fedo, C. M., and Young, G. M., 1997. Quartz and feldspar stability, steady and non-steady-state weathering and petrogenesis of siliciclastic sands and muds. J. Geol., 105: 173-191.

Powell, C. McA., et. al., 1994. South Australian record of a Rodinian epicontinental basin and its Mid-Neoproterozoic breakup to the Paleo-Pacific ocean. Tectonophys., 237: 113-140.

Roser, B. P. and Korsch, R. J., 1988. Provenance signatures of sandstone-mudstone suites determined using discriminant function analysis of major-element data. Chem. Geol., 67: 119-139.

Rosholt, J. N., 1983. Isotopic composition of uranium and thorium in crystalline rocks. J. Geophys. Res., 88: 7315-7330.

Sanderson, I. D., 1979. Sedimentology and paleoenvironments of the Mt. Watson Formation, Upper Precambrian Uinta Mountain Group, Utah. Ph. D. dissert., Univ. Colorado, 150 pp.

Sanderson, I. D., 1984. The Mt Watson Fm, and interpreted braided-fluvial deposit in the Uinta Mountain Group, Utah. Mountain Geol., 21 (4): 157-164.

Sanderson, I. D. and Wiley, M. T., 1986. The Jesse Ewing Canyon Fm, and interpreted alluvial fan deposit in the basal Uinta Mountain Group, Utah. Mountain Geol., 23(3): 77-89.

Sawyer, E. W., 1986. The influence of source rock type, chemical weathering and sorting on the geochemistry of clastic sediment from the Quetico metasedimentary belt, Superior province, Canada. Chemical Geol., 55: 77-95.

Schwab, F., 1998. Middle to late Proterozoic sedimentary tectonic framework of the western and SW US: insights from the Uinta Mountain Group. Geol. Soc. Amer., Abst. With Programs, 29(6): 35-36.

Sears, J. W., Graff, P. S. and Holder, G. S., 1982. Tectonic evolution of Lower Proterozoic rocks, Uinta Mountains, Utah and Colorado. Geol. Soc. America Bull., 93: 990-997.

Stuckless, J. S., 1989. Petrogenesis of two contrasting, Late Archean granitoids, Wind River Range, Wyoming. U. S. Geol. Survey, Prof. Paper 1491, 38 p.

Stuckless, J. S., Sunker, C. M., Bush, C. A., Doering, W. P., and Scott, J. H., 1977. Geochemical and petrological studies of the uraniferous granite from the Granite Mountains, Wyoming. J. Res. U. S. Geol. Surv., 5 (1): 61-81.

Taylor, S. R. and McLennan, S. M., 1985. The Continental Crust: Its Composition and Evolution. London, Blackwell Scientif. Pub., 312 pp.

Vidal, G., 1985. Microbiotas from the Late Proterozoic Chuar Group and Uinta Mountain Group and their chronostratigraphic implications. Precamb. Res., 28: 349-389.

Wallace, C. A. and Crittenden, Jr., M. D., 1969. The stratigraphy, depositional environment and correlation of the Precambrian Uinta Mountain Group, Western Uinta Mountains, Utah. Geologic Guidebook of the Uinta Mountains, Intermount. Assoc. Geol., 16th Field Conf.

Wooden, J. L. and Mueller, P. A., 1988. Pb, Sr, and Nd isotopic compositions of a suite of Late Archean igneous rocks, eastern Beartooth Mountains: implications for crust-mantle evolution. Earth Planet. Sci. Lettr., 87: 59-72.

APPENDIX A: PETROGRAPHY

Hades Peak Formation Sample #2.
Little Deer Creek near juncture with Duchesne River.

Quartz-arenite. Brown clay weathering rind, massive bedding, 10 cm thick.
Red-gray, fine to medium grained, well-sorted, well-rounded, well indurated, quartz cement. 10% of cementation is calcite infilling.
95% quartz, very well-rounded, very well-sorted, fine to medium grained.
5% palgioclse, angular to subangular, medium grained, untwinned.
This sample has the distinct feature, in this study, of secondary calcite cementation within predominately silica cement. Where calcite has replaced or infilled voids can be seen as lineations in the slide. Individual quartz grains appear to drift into calcite cement from quartz cemented sections.

Hades Peak Formation Sample #4.
Cobble Rest Campground, HWY 150, across the road from campground.

Quartz-arenite. Whitish-brown clay weathering rind, massive bedding, 70 cm thick.
Pinkish, red-gray, fine to medium grained, well-sorted, well-rounded, quartz cement.
96% quartz, well-rounded, well-sorted, fine to medium grained. Grain compaction between quartz grains. Well defined grain boundaries high-lighted by dark clay coating on grains.
4% potassium feldspar, angular to subangular, medium grained.

Hades Peak Formation Sample #5.
Cobble Rest Campground, HWY 150, across the road from campground.

Quartz-arenite. Dark brown clay weathering rind, massive bedding, 50 cm thick.
Pink-red, fine to medium grained, well-sorted, well-rounded, quartz cement.
97% quartz, well-rounded, well-sorted, fine to medium grained. 1-2% quartz is polyquartz, with sutured boundaries, well-rounded, medium grained.
1% chert fragments, well-rounded, medium sized
1% potassium feldspar, angular to subangular, medium grained.
trace amounts of biotite.

Hades Peak Formation Sample #13.
Scow Creek, on trial 500 meters south of Scow Lake.

Arkose. Tan-brown clay weathering rind, cross-bedding, 150 cm thick.
Pink-red, medium to coarse grained, poor to moderately sorted, well-rounded, quartz cement.
55% quartz, 40% detrital, well-rounded, well-sorted, fine grained, 15% polygrained metaquartzite, sutured boundaries, medium to coarse grained.
26% potassium feldspar, medium to coarse grained, angular to sub-angular.
18% plagioclase, medium grained, angular, twinned and untwinned, some alteration to sericite.

Hades Peak Formation Sample #14.
Iron Mine Creek, cliff adjacent to creek, 1/3 way up.

Quartzite. White, massive,1 meter thick.
White, fine grained, well sorted, well rounded, indurated, quartz cement.
100% quartz, 97% detrital, well-rounded, well-sorted, fine grained, 3% polygrained metaquartzite, sutured boundaries, medium to coarse grained.
several zircons identified in sample.

Hades Peak Formation Sample #18.
Whiskey Island Lake, cliff face adjacent to lake, 1/2 way up.

Quartz-arenite. White, cross bedded, 50 cm thick.
White, fine to very fine-grained, well sorted, well rounded, indurated, quartz cement.
92% quartz, detrital, well rounded, well sorted, fine grained,
6% potassium feldspar, medium grained, angular to subangular.
2% plagioclase, untwinned, fresh, no alteration.

Hades Peak Formation Sample #21.
Whiskey Island Lake, cliff face adjacent to lake, 3/4 way up.

Quartz-arenite. Brown, massive, 70 cm thick.
Pinkish-red, fine to medium grained, well sorted, well rounded, indurated, quartz cement. Bimodal from rounded, fine grained quartz and medium to coars grained polycrystalline quartz, potassium feldspar, and plagioclase
91% quartz, detrital, well rounded, well sorted, fine grained,
2% polycrystalline quartz, medium grained, sutured boundaries, angular.
3% potassium feldspar, medium to coarse grained, angular to subangular.
2% plagioclase, some alteration with sericite, twinning.

Hades Peak Formation Sample #22.
Whiskey Island Lake, cliff face adjacent to lake, near the top.

Quartz-arenite. Light brown, cross bedded, 50 cm thick.
Reddish-pink, fine to very fine grained, well sorted, well rounded, indurated, quartz cement.
95% quartz, detrital, well rounded, well sorted, fine grained,
5% chert fragments, well rounded medium grained

Hades Peak Formation Sample #24.
Fish Lake, north-west cliff face adjacent to lake, near the bottom of cliff.

Arkose. Tan-brown, massive bedded, 80 cm thick.
White-pink, medium to coarse grained, poor to moderately sorted, angular to sub-angular, hard, clay matrix.
60% monocrystalline quartz, detrital, well rounded, well sorted, fine grained
12% polycrystalline quartz, sutured boundaries, medium grained, subangular
18% potassium feldspar, subrounded to angular, medium to coarse grained
10% plagioclase, medium to fine grained, angular, some altered almost entirely to sericite.
trace chert fragments, well rounded, fine grained

Hades Peak Formation Sample #25.
Fish Lake, west cliff face adjacent to lake, near the bottom of cliff, on the trail.

Arkose. Reddish-brown, massive bedded, 60 cm thick.
reddish-pink, medium to coarse grained, poor to moderately sorted, angular to sub-angular, hard, clay matrix, clay coating on grains
78% monocrystalline quartz, detrital, well rounded, well sorted, fine to medium grained.
3% polycrystalline quartz, sutured boundaries, medium grained, subangular
2% potassium feldspar, subrounded to angular, medium to coarse grained
8% plagioclase, medium to fine grained, angular, some altered to sericite.
9% chert and transported quartz arenite, well rounded, fine-medium grained. Recycled quartz lithic fragments are medium to coarse, angular to subangular, quartz cemented, containing fine grained, well rounded quartz arenite.

Mount Watson Formation Sample #2.
Highway 150, near Mile Marker 38

Arkose. Brownish-red, cross bedded, 50 cm thick.
Red-pink, fine to coarse grained, poorly sorted, angular, hard, hematite matrix, clay coating on grains
34% monocrystalline quartz, detrital, well rounded, well sorted, fine to medium grained, undulatory
10% polycrystalline quartz, sutured boundaries, medium grained, angular
13% potassium feldspar, subrounded to angular, coarse grained
43% plagioclase, medium to fine grained, angular, some altered to sericite, predominately twinned grains.

Mount Watson Formation Sample #10.
West Hayden Peak, up from Hayden Pass trail head parking on Highway 150

Subarkose. Brownish-red, cross bedded, 50 cm thick.
Red-pink, fine to coarse grained, poorly sorted, angular, hard, hematite matrix, clay coating on grains
83% monocrystalline quartz, detrital, well rounded, well sorted,
13% potassium feldspar, subrounded to angular, coarse grained
43% plagioclase, medium to fine grained, angular, some altered to sericite, predominately twinned grains.

Mount Watson Formation Sample #11.
West Hayden Peak, up from Hayden Pass trail head parking on Highway 150

Arkose. Brownish-red, cross bedded, 50 cm thick.
Red-pink, fine to coarse grained, poorly sorted, angular, hard, quartz cement
54% monocrystalline quartz, detrital, well rounded, well sorted,
12% polycrystalline quartz, medium grained, sutured boundaries
22% potassium feldspar, subrounded to angular, coarse grained
10% plagioclase, medium to fine grained, angular, some altered to sericite, predominately twinned grains.

Mount Watson Formation Sample #24.
A-1 Peak, east side, accessed via West Basin Trail off of Stillwater Fork south of Christmas Meadows.

Arkose. Tan-brown clay weathering rind, cross-bedding, 2 meters thick.
Pink-red, medium to coarse grained, poor to moderately sorted, well-rounded, quartz cement.
25% monocrystalline quartz, detritital, well-rounded, well-sorted, fine grained, 26% polygrained metaquartzite, sutured boundaries, medium to coarse grained, angular
19% potassium feldspar, medium to coarse grained, angular to sub-angular.
30% plagioclase, medium grained, angular, twinned and untwinned, some alteration to sericite.

Mount Watson Formation Sample #27.
A-1 Peak, east side, accessed via West Basin Trail off of Stillwater Fork south of Christmas Meadows.

Quartz arenite. Tan, massive bedded, 1 meter thick.
Light red-pinkish, fine to medium grained, well sorted, well rounded, indurated, quartz cement
97% monocrystalline quartz, detrital, well rounded, well sorted, grain compaction.
2% potassium feldspar, subrounded to angular, coarse grained
1% plagioclase, medium to fine grained, angular, some altered to sericite, predominately twinned grains.

Mount Watson Formation Sample #37.
Kamas Lake, north side.

Quartz arenite. Yellowish-brown, massive bedded, 1 1/2 meters thick.
Light red, fine to medium grained, well sorted, well rounded, indurated, quartz cement
91% monocrystalline quartz, detrital, well rounded, well sorted, grain compaction.
2% polycrystalline quartz, medium grained, sutured boundaries
4% potassium feldspar, subrounded to angular, coarse grained
3% plagioclase, medium to fine grained, angular, some altered to sericite, predominately twinned grains.

Mount Watson Formation Sample #41.
Cuberant Lake, north side, bottom of cliff

Subarkose. Light brown, massive bedded, 2 meters thick.
Light red, medium to coarse grained, moderately sorted, angular to subangular, indurated, quartz cement
81% monocrystalline quartz, detrital, very well rounded, well sorted, grain compaction.
8% polycrystalline quartz, medium grained, sutured boundaries
8% potassium feldspar, subrounded to angular, coarse grained, one k-spar grain measuring 1/2 cm
3% plagioclase, medium to fine grained, angular, some altered to sericite, twinned grains.

Mount Watson Formation Sample #48.
Lamotte Peak, south west, midway up cliff, reached via Ostler Fork.

Arkose. Light gray, massive bedded, 1 meter thick.
Gray, medium to coarse grained, poorly sorted, sub-rounded to angular, indurated, quartz cement. Strikingly absent in potassium feldspar.
18% monocrystalline quartz, detrital, very well rounded, well sorted, grain compaction.
40% polycrystalline quartz, medium grained, sutured boundaries, undulatory extinctions
42% plagioclase, medium to fine grained, angular, some altered to sericite, twinned grains.

Mount Watson Formation Sample #49.
Lamotte Peak, south west, midway up cliff, reached via Ostler Fork.

Quartz arenite. Light gray, massive bedded, 1 meter thick.
Gray, fine grained, very well sorted, well rounded, indurated, quartz cement. 100% monocrystalline quartz, detrital, very well rounded, well sorted, grain compaction.

Red Castle Formation Sample #2.
West Basin Creek, cliff face in gorge formed by creek.

Arkose. Light brown, cross bedded, 2 meters thick.
Pinkish-red, coarse grained, poorly sorted, sub-rounded to angular, indurated, quartz cement.
26% monocrystalline quartz, detrital, fine to medium, well rounded, moderately sorted.
29% polycrystalline quartz, coarse grained, sutured boundaries, undulatory extinctions
20% potassium feldspar, coarse grained, angular, subangular
26% plagioclase, medium to fine grained, angular, some altered to sericite, twinned grains.

Red Castle Formation Sample #7.
West Basin Creek, cliff face in gorge formed by creek.

Arkose. Light brown, massive, 3 meters thick.
Gray, medium to coarse grained, moderately to poorly sorted, sub-rounded to angular, indurated, quartz cement.
27% monocrystalline quartz, detrital, fine to medium, well rounded, moderately sorted.
14% polycrystalline quartz, coarse grained, sutured boundaries, undulatory extinctions
26% potassium feldspar, coarse grained, angular, subangular
33% plagioclase, medium to fine grained, angular, some altered to sericite, twinned grains.

Red Castle Formation Sample #9.
West Basin Creek, cliff face in gorge formed by creek.

Quartz arenite. Light gray, massive bedded, 1 meter thick.
Gray, fine grained, very well sorted, well rounded, indurated, quartz cement. 96% monocrystalline quartz, detrital, very well rounded, well sorted, grain compaction.
3% plagioclase, medium to fine grained, angular, some altered to sericite.

Red Castle Formation Sample #10.
West Basin Creek, cliff face in gorge formed by creek.

Subarkose. Light brown, massive, 3 meters thick.
Gray, medium to coarse grained, moderately to poorly sorted, sub-rounded to angular, indurated, quartz cement.
91% monocrystalline quartz, detrital, fine to medium, well rounded, moderately sorted.
5% potassium feldspar, coarse grained, angular, subangular
3% plagioclase, medium to fine grained, angular, some altered to sericite, twinned grains.

Uinta Mountain Group Undifferentiated Sample #1, #2, #3.
Gorge in the East Fork of the Duchesne River near juncture with Marshall Canyon.

Quartz arenite. Light gray, cross bedded, 1 meter thick.
White-gray, fine grained, very well sorted, well rounded, indurated, quartz cement.
100% monocrystalline quartz, detrital, very well rounded, well sorted.

APPENDIX B: WHOLE ROCK CHEMISTRY

	RP-1	RP-3	RP-4	RP-9	RP-17	RP-20
SiO2	57.51	52.81	51.59	54.44	62.89	61.56
TiO2	0.95	1.1	1.19	1.05	0.92	0.89
Al2O3	19.03	22.49	23.21	24.73	16.63	16.69
Fe2O3T	8.32	7.48	7.49	5.28	1.58	2.09
MgO	2.6	3.04	2.92	1.86	0.92	1.02
CaO	0.54	0.5	0.33	0.31	0.09	0.11
Na2O	1.71	0.9	0.26	0.72	0.91	0.91
K2O	2.49	3.41	4.91	3.47	3.76	4.44
MnO	0.03	0.02	0.025	0.018	0.005	0.014
P2O5	0.12	0.16	0.14	0.21	0.09	0.11
LOI	6.85	7.64	7.48	7.61	11.53	10.62
Total	100.15	99.55	99.545	99.698	99.325	98.454
Rb	115	116	136	138	147	159
Sr	103	161	125	185	98	94
Ba	753	264	446	329	412	380
Th	36	16	19	41	27	24
U	6	5	5	11	8	7
Pb	49	13	40	28	14	20
Zr	219	233	249	307	247	249
Hf	6.83	8.85	8.1	9.22	7.25	9.2
Ta	1.97	1.3	1.35	1.92	1.93	1.9
Nb	23	14	18	25	24	24
La	69.7	65.1	66.6	104.7	81	79.4
Ce	130	135.9	137.9	211.1	155.9	158.4
Nd	55	56.3	49.2	80	63	69
Sm	9.32	11.48	12.05	12.74	11.67	11.96
Eu	1.43	2.38	2.26	1.95	1.86	1.9
Gd	6.8	10.1	9.3	9.1	9.7	9.5
Tb	0.94	1.53	1.32	1.25	1.44	1.37
Yb	3.37	4.5	4.8	4.65	4.47	4.5
Lu	0.506	0.659	0.668	0.679	0.689	0.633
Y	34	49	47	46	50	49
V	84	177	177	102	119	113
Sc	14.0	24.0	24.8	16.8	13.9	14.0
Cr	95.1	130	138.8	93.2	94.7	89.3
Co	17.7	32.1	28.4	11.5	6.2	8.8
Ni	56	68	76	38	17	17
CIA	75.4	79.8	79.4	83.2	75.1	72.8
Eu/Eu*	0.55	0.68	0.66	0.56	0.54	0.55
(Gd/Yb)n	1.62	1.80	1.55	1.58	1.75	1.70

	HP-1	HP-8	HP-28	MW-25	MW-47	MW-50
SiO2	60.44	69.62	73.2	57.54	69.49	60.33
TiO2	0.96	0.81	0.85	0.98	0.77	0.94
Al2O3	20.98	14.89	14.41	20.35	15.19	19.54
Fe2O3T	4.97	4.85	4.55	5.93	5.18	7.14
MgO	1.21	1.27	1.47	2.87	1.25	1.83
CaO	0.1	0.11	0.17	0.21	0.12	0.19
Na2O	0.07	0.07	0.14	1.44	0.08	0.17
K2O	5.63	3.97	4.28	6.21	3.82	3.93
MnO	0.037	0.073	0.014	0.026	0.014	0.019
P2O5	0.1	0.06	0.05	0.11	0.05	0.08
LOI	5.18	4.3	0.71	4.01	3.73	5.91
Total	99.677	100.02	99.844	99.676	99.694	100.08
Rb	172	142	135	243	136	160
Sr	74	46	55	107	42	53
Ba	322	227	360	539	357	817
Th	25	13	22	48	17	31
U	8	4	6	9	4	9
Pb	23	17	18	42	14	20
Zr	327	423	525	400	384	301
Hf	9.9	12.9	10	12	11.85	8.65
Ta	1.67	1.48	1.4	2.49	1.78	1.79
Nb	21	15	15	25	16	23
La	67.5	39.8	39.9	104.6	42.7	81.1
Ce	132.1	78.9	79.8	201.6	86.3	162.4
Nd	47.7	32.5	31.5	67	37.3	68
Sm	9.84	6.28	5.47	10.25	6.9	12.11
Eu	1.53	1.1	0.95	1.59	1.16	2.01
Gd	8.0	5.5	5.0	8.1	6.1	9.8
Tb	1.17	0.84	0.77	1.16	0.93	1.42
Yb	4.42	3.3	3.04	4.28	3.29	4.27
Lu	0.587	0.471	0.5	0.64	0.49	0.612
Y	43	31	27	44	31	47
V	90	83	75	57	78	92
Sc	15.7	13.0	11.3	14.4	12.4	15.9
Cr	84.4	79.3	95	56.4	76.8	102.8
Co	25.4	30.2	15.2	36.4	44.5	19.5
Ni	35	28	32	42	35	52
CIA	77.3	76.9	74.0	68.8	77.7	80.6
Eu/Eu*	0.53	0.57	0.56	0.54	0.55	0.57
(Gd/Yb)n	1.46	1.35	1.32	1.52	1.49	1.84

	RC-6	RC-8	MHL-6	MHL-12	MHL-15	BC-1A
SiO2	63.84	58.9	68.43	58.63	64.87	59.69
TiO2	0.92	0.94	0.87	0.98	0.97	0.93
Al2O3	17.92	19.12	18.24	21.39	20.39	22.36
Fe2O3T	5.85	7.66	3.22	7.22	2.93	6.17
MgO	1.63	2.59	0.99	1.5	1.04	1.58
CaO	0.13	0.16	0.02	0.14	0.16	0.06
Na2O	0.09	1.29	0.09	0.35	0.54	0.53
K2O	4.52	4.51	3.41	4	3.03	3.9
MnO	0.02	0.025	0.009	0.016	0.011	0.019
P2O5	0.06	0.1	0.05	0.06	0.05	0.07
LOI	4.5	4.38	4.92	6.02	5.86	4.71
Total	99.48	99.675	100.25	100.31	99.851	100.02
Rb	156	163	130	195	125	181
Sr	58	70	42	64	49	76
Ba	522	418	238	529	540	503
Th	32	54	14.8	32	26	19
U	9	13	4.6	7	9	6
Pb	14	24	13	21	18	17
Zr	417	400	382	271	357	221
Hf	13.5	12.3	12.2	8.01	11.1	6.7
Ta	2.08	2.33	1.43	1.85	1.92	1.5
Nb	21	23	18	21	21	18
La	71.5	90.1	43.7	90	76.3	64
Ce	129.1	181.6	84.7	162.8	141.1	144.8
Nd	58	71	33.3	58	44.5	58.3
Sm	9.85	12.79	6.33	9.89	7.4	10.4
Eu	1.44	2.04	0.96	1.44	1.28	2.14
Gd	8.3	9.2	5.6	7.6	5.9	7.6
Tb	1.23	1.27	0.85	1.08	0.85	1.41
Yb	3.97	3.09	3.62	4.18	3.7	4.2
Lu	0.556	0.458	0.5	0.591	0.577	0.663
Y	50	35	34	41	33	42
V	91	108	93	95	98	137
Sc	14.2	14.5	15.0	17.5	17.1	24.0
Cr	81.2	68	85.1	93.3	94.9	133
Co	36.4	36.7	11.2	23.1	18.8	25.0
Ni	37	51.8	25	41	30	51
CIA	77.7	73.0	82.9	81.0	82.4	81.6
Eu/Eu*	0.49	0.58	0.50	0.51	0.60	0.74
(Gd/Yb)n	1.68	2.40	1.24	1.46	1.28	1.46

	BC-6B	BC-8A
SiO2	63.46	68.05
TiO2	1	0.99
Al2O3	22.38	16.05
Fe2O3T	3.41	7.2
MgO	0.89	0.94
CaO	0.05	0.13
Na2O	0.48	1.19
K2O	3.43	2.81
MnO	0.021	0.029
P2O5	0.05	0.11
LOI	4.68	2.49
Total	99.851	99.989
Rb	153	122
Sr	80	60
Ba	557	545
Th	17	16
U	5	5
Pb	11	22
Zr	291	430
Hf	8.82	13
Ta	1.4	1.5
Nb	17	18
La	65	61
Ce	147	133.8
Nd	61.8	63
Sm	12.13	10.3
Eu	1.76	1.93
Gd	7.2	5.9
Tb	1.63	1.5
Yb	4.1	4
Lu	0.68	0.67
Y	40	41
V	125	108
Sc	21.6	17.0
Cr	129	104
Co	15.3	18.2
Ni	35	44
CIA	83.3	76.3
Eu/Eu*	0.58	0.76
(Gd/Yb)n	1.41	1.19

	HP-2	HP-4	HP-5	MW-10	MW-37	MW-41
SiO2	93.42	97.46	98.75	94.46	97.08	94.47
TiO2	0.07	0.04	0.08	0.06	0.04	0.04
Al2O3	0.82	0.85	0.58	3.38	0.98	3.01
Fe2O3T	2.19	0.65	0.33	0.19	0.05	0.37
MgO	0.61	0.09	0.07	0.1	0.05	0.14
CaO	0.01	0.03	0.02	0.03	0.01	0.03
Na2O	0.03	0.03	0.02	0.45	0.085	0.58
K2O	0.36	0.37	0.23	1.52	0.41	1.22
MnO	0.13	0.003	0.002	0.0035	0.002	0.004
P2O5	0.02	0.02	0.02	0.02	0.026	0.02
LOI	1.78	0.25	0.17	0.38	0.17	0.35
Total	99.44	99.79	100.27	100.59	98.90	100.23
Rb	7	14	6	38	9	32
Sr	22	26	22	20	10	16
Ba	19	65	32	238	58	156
Th	2.0	3.0	4.0	2.8	2.5	3.0
U	1.5	1	0.8	0.9	0.75	1
Pb	3	1	2	3	1	2
Zr	55	38	109	62	54	40
Hf	1.8	2.5	3.14	1.51	1.7	2.79
Ta	1.61	1.84	2.09	1.44	2.44	1.82
Nb	2.0	1.9	2.1	1.8	2.5	1.7
La	6.0	4.6	7.1	8.1	4.1	6.2
Ce	10.0	9.7	13.3	12.5	6.8	10.1
Nd	4.0	5.5	4.0	4.7	3.7	3.6
Sm	0.64	0.78	0.94	0.75	0.57	0.56
Eu	0.13	0.11	0.16	0.15	0.09	0.13
Gd	1.24	1.35	1.55	0.80	1.02	0.84
Tb	0.1	0.3	0.3	0.1	0.1	0.1
Yb	0.31	0.47	0.38	0.25	0.24	0.25
Lu	0.05	0.06	0.06	0.03	0.02	0.03
Y	7.0	4.0	4.0	3.0	2.0	3.0
V	17	12	10	7	7	6
Sc	0.4	0.4	0.5	0.4	0.2	0.3
Cr	10.5	15.6	9.2	5.2	5.2	7.2
Co	81	91	95	66	127	84
Ni	4.0	4.0	3.0	3.0	3.0	4.0
CIA	66.7	65	68.2	58.6	64.5	56.9
Eu/Eu*	0.45	0.32	0.41	0.59	0.37	0.59
(Gd/Yb)n	3.20	2.31	3.27	0.56	3.48	2.66

	RC-9	RC-10	UMG-1	HP-6	HP-31	HP-24
SiO2	95.96	95.04	99.14	83.89	83.68	86.63
TiO2	0.11	0.05	0.04	0.33	0.19	0.09
Al2O3	0.97	2.58	0.55	6.79	9.23	5.77
Fe2O3T	0.27	0.31	0.08	4.59	1.57	0.22
MgO	0.15	0.26	0.04	0.74	0.58	0.21
CaO	0.02	0.05	0.01	0.11	0.23	0.04
Na2O	0.08	0.5	0.03	0.04	3.29	0.4
K2O	0.25	0.70	0.15	1.35	0.76	2.92
MnO	0.002	0.003	0.002	0.0065	0.0085	0.002
P2O5	0.02	0.028	0.02	0.11	0.035	0.02
LOI	0.28	0.54	0.15	1.93	0.5	3.61
Total	98.11	100.06	100.21	99.89	100.07	99.91
Rb	8	20	4	43	26	74.00
Sr	10	19	14	57	53	37
Ba	24	410	15	829	161	348
Th	2.0	1.0	1.0	6.0	6.0	14.0
U	0.85	0.6	0.5	4	2	2
Pb	0	1	1	20	2	5
Zr	240	61	40	263	86	119
Hf	9.64	1.63	0	7.7	2.53	4.04
Ta	3.64	1.63	3.83	1.23	1.13	1.73
Nb	2.0	2.1	2.0	6.0	4.0	3.0
La	6.9	7.1	5.2	18.9	12.0	17.8
Ce	13.7	11.0	9.0	40.3	22.1	33.5
Nd	5.3	4.5	4.9	15.0	9.5	10.1
Sm	1.09	0.87	0.87	3.61	2.49	2.18
Eu	0.18	0.15	0.14	0.71	0.48	0.35
Gd	1.02	1.14	0.77	3.26	1.93	2.90
Tb	0.2	0.2	0.1	0.5	0.3	0.54
Yb	0.64	0.26	0.22	1.34	0.66	0.78
Lu	0.11	0.04	0.03	0.19	0.09	0.12
Y	5.0	3.0	2.0	14.0	9.0	15.0
V	12	6	4	50	32	13
Sc	0.6	0.3	0.2	4.3	2.0	1.0
Cr	6.3	6.8	5.3	30.3	6.6	6.2
Co	184	84	200	46	54	80
Ni	4.0	3.0	3.0	22.0	18.0	5.0
CIA	71.3	61.7	75.1	82.2	58.4	60
Eu/Eu*	0.52	0.46	0.52	0.64	0.67	0.43
(Gd/Yb)n	1.27	3.51	2.84	8.55	2.35	2.99

	MW-2	MW-11	MW-29	RC-2	RC-4	RC-7
SiO2	78.3	89.09	82.05	83.4		75.11
TiO2	0.35	0.04	0.11	0.14	0.37	0.34
Al2O3	10.91	5.95	9.72	9.58	6.43	12.37
Fe2O3T	3.53	0.36	1.5	0.38	3.09	3.98
MgO	0.53	0.09	0.28	0.18	0.63	0.97
CaO	0.28	0.08	0.12	0.1	0.06	0.19
Na2O	2.92	1.35	2.76	2.66	0.31	2.93
K2O	2.30	2.72	3.15	3.23	2.21	3.61
MnO	0.017	0.004	0.006	0.013	0.006	0.01
P2O5	0.04	0.02	0.02	0.03	0.03	0.05
LOI	0.29	0.6	1.07	0.59	1.26	1.24
Total	99.47	100.30	100.79	100.30	100.42	100.80
Rb	74	64	81	85	70	
Sr	108	36	55	49	27	71
Ba	865	424	579	725	185	
Th	7.0	8.0	10.0	9.0	5.0	4.0
U	3	1	1	1	2	1.1
Pb	12	5	9	5	13	
Zr	111	37	73	63	303	184
Hf	3.57	0.65	1.96	1.8	9.83	4.8
Ta	1.08	1.93	1.24	1.63	1.76	3.1
Nb	4.5	2.2	3.0	4.0	5.0	8.0
La	15.2	7.6	19.0	26.2	19.8	30.0
Ce	31.4	11.4	29.3	42.7	40.5	51.2
Nd	12.8	5.6	10.0	14.1	16.9	19.5
Sm	3.16	0.70	1.57	1.99	2.96	3.25
Eu	0.61	0.11	0.33	0.25	0.53	0.57
Gd	2.40	1.28	1.03	1.46	3.21	2.77
Tb	0.3	0.3	0.1	0.2	0.5	0.4
Yb	0.20	0.41	0.61	0.41	1.59	1.37
Lu	0.03	0.06	0.09	0.06	0.23	0.21
Y	11.0	3.0	6.0	6.0	15.0	13.0
V	56	12	17	15	25	23
Sc	0.4	1.4	1.6	1.7	4.7	4.2
Cr	7.1	6.6	9.6	6.7	37.7	32.0
Co	87	52	49	65	60	60
Ni	4.0	5.0	7.0	7.0	34.0	10.0
CIA	58.6	53.1	54.5	54.5	68.6	58
Eu/Eu*	0.68	0.36	0.80	0.45	0.53	0.58
(Gd/Yb)n	9.48	2.50	1.36	2.86	1.63	1.62

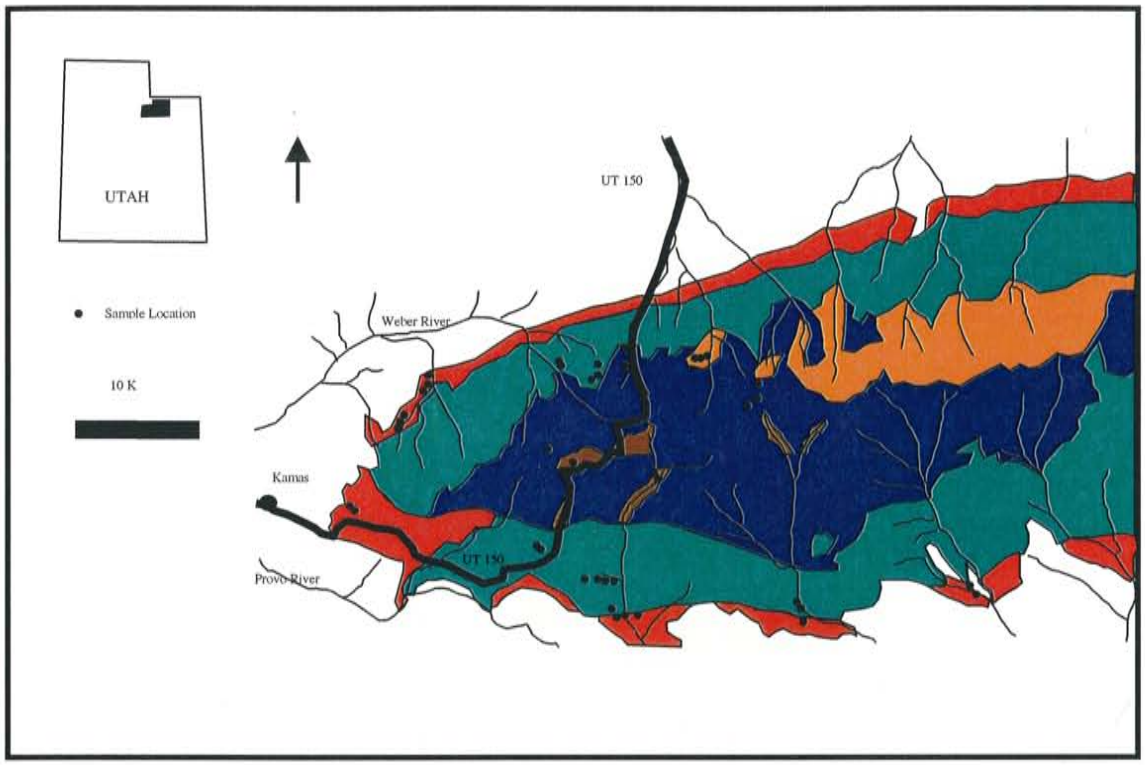

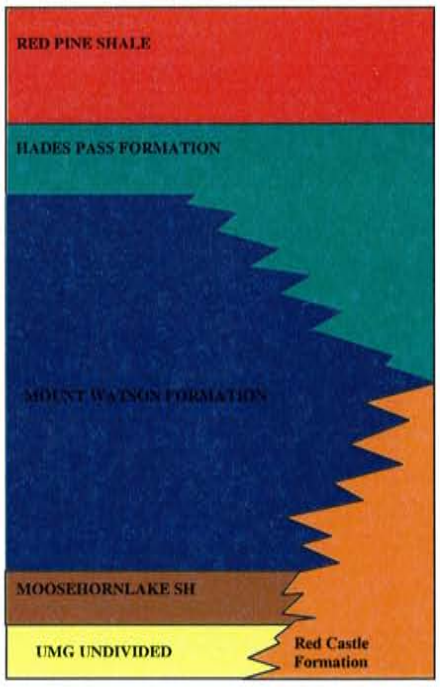

Figure21: Geology of the Uinta Mountain Group. Above is a map showing the location of the study area. Below is a generalized section of the members in the western UMG. Sample locations for this study are indicated on the map.